12-2018

Using Contraflow on a Road Segment to Improve Emergency Response Vehicle Speed in a Connected Vehicle Environment

Nitin Srinath
Clemson University, nitin.carfan@gmail.com

USING CONTRAFLOW ON A ROAD SEGMENT TO IMPROVE EMERGENCY RESPONSE VEHICLE SPEED IN A CONNECTED VEHICLE ENVIRONMENT

A Thesis
Presented to
the Graduate School of
Clemson University

In Partial Fulfillment
of the Requirements for the Degree
Master of Science
Industrial Engineering

---

by
Nitin Srinath
December 2018

Accepted by:
Dr. Sandra D Eksioglu, Committee Chair Dr.
Pamela Marie Murray-Tuite, Co-Chair
Dr. J. Cole Smith

ABSTRACT

Emergency response vehicles (ERVs) need to reach their destinations as fast as possible. Road congestion and unpredictable movement of non-emergency vehicles (non-ERVs) makes it challenging for the ERV to move quickly. By using the autonomous/connected vehicle environment, instructions can be disseminated to the non-ERVs in the vicinity of the ERV to facilitate its passage within a link. In this thesis, an extension to a previously developed mathematical program is proposed to enable the ERV to use a contraflow lane when considerable speed gains can be potentially achieved. An experimental analysis is conducted to evaluate the sensitivity of the model's output to traffic congestion, downstream non-ERV positions, ERV starting position, road composition, road segment length, and the length of the feasible stopping range for every non-ERV. Results showed that usage of contraflow was provided the least travel times for the ERV when it started in the left-most lane of the normal direction. Also, when the normal direction of the road was heavily congested as compared to the contraflow segment, the usage of contraflow by the ERV provided it the least travel times. In addition, a comparative study is performed to compare the proposed formulation with previously developed non-contraflow strategies as well as a the currently adopted strategy requiring vehicles to move to the nearest edge. Results showed that the use of contraflow by the ERV provides improved travel times and average ERV speeds in many situations when the contraflow segment volume was sparse whereas the normal direction was congested. However, the computation times for the newly developed contraflow strategy were greater than the previously developed non-contraflow strategies. So, a heuristic was developed to

reduce computational effort by cutting off the solver at a specified point, which was decided by how far the current feasible solution found was from the possible optimal solution (optimality gap). This heuristic not only provided improved computation times, but also results which did not statistically differ from the optimal results. The paths provided by the heuristic were also similar with the only difference being the points at which the lane changes happened. Hence, the utilization of this approach can potentially save lives due to reduced emergency response times.

TABLE OF CONTENTS

CHAPTER ONE

INTRODUCTION

Emergency vehicles' response times need to be as short as possible. These times significantly affect mortality in emergency medical situations. Results from a study in the state of Utah have shown that a minute increase in travel time increased mortality by 8-17%. Response times tend to be even more critical towards the mortality rate when age is a factor [1]. It is important to devise ways to reduce response times. From a study conducted in the urban area of Charlotte, NC, there is a significant rise in survivals when the response times are less than 5 minutes in emergency medical systems [2]. Specifically, in a survey of cardiac arrests conducted in Scotland, reduced response times greatly affected the chances of a patient receiving medical treatment in time to survive. Only a 9-minute reduction in response time increased the rate of survival by about 11% [3]. A comprehensive analysis of multiple studies pertaining to medical emergencies and emergency service response times conclude that every minute counts towards reducing the mortality risk, and there indeed is a significant difference in survival rates where response time is a factor [4].

Road congestion and traffic movement poses a major challenge when trying to reduce the response time of an emergency vehicle. If there was a way to control the flow of traffic and the movement of vehicles on the road, it would give us opportunities to move vehicles such that the response time of the emergency vehicle (ERV) could be reduced greatly. This forms the basis of this thesis. While it is indeed hard to control the motion of every single vehicle on the road today, it is one of the major advantages of autonomous and connected vehicle systems.

Autonomous and connected vehicle environments offer new opportunities to develop (potentially safer) strategies to facilitate emergency response vehicle (ERV) movement. In this thesis, initial work developed in [5] is extended, by allowing the ERV to use a lane from the opposing direction when there are no physical barriers preventing that movement.

Contraflow strategies have reduced travel times in several situations, such as evacuation [7, 8] and transit plans in emergency situations [9]. Use of contraflow strategies provided an improvement of about 9.8%, with delays reduced by 34% and average speed of traffic increasing by 16% in a study conducted for evacuation strategies in the state of Texas. When contraflow was used, there was a 13% increase in the total number of evacuees moving from a danger zone to a safe zone [7]. In a study comparing different strategies employed during evacuation [8], the contraflow strategy provided the most significant reduction in evacuation time. However, opposing traffic poses a safety concern and the communication among vehicles is critical, especially when physical barriers between the opposing flows are not implemented.

To maximize the speed of the ERV through a two-way road segment, we revised and extended the initial integer linear program developed in [5]. Inputs to this mathematical model are the initial positions and speeds of all vehicles on the road segment in both directions, along with their deceleration capabilities. We also take into consideration the road composition and presence of a raised median. The formulation is coded and solved using the commercially available solvers Gurobi/CPLEX. The outputs of the model include stopping positions of the non-ERVs in addition to the speed and intra-link path of the ERV.

The formulation is tested under a variety of conditions. These include different road compositions, initial speeds of the ERV and non-ERVs, position of the ERV initially, traffic densities on both sides of the road, length of the road segment and length of the feasible stopping ranges for every non-ERV.

We also performed tests on computation time, because this is a major factor when considering the practicality of the strategy. Since we are working with moving vehicles on the road, computation times must be very low to send route and movement instructions to the vehicles. Tests are conducted with parameters as the length of optimized road segment and feasible stopping ranges for the non-ERVs, and conclusions about the computation times are drawn.

Next, we conducted comparison tests between the newly developed contraflow strategy and the previously developed non-contraflow strategy and analyzed the benefits, if any. We also analyzed the improvements of using the contraflow strategy over the current practice of moving vehicles to the nearest edge in the presence of an emergency vehicle.

While the results from the tests conducted showed improvement over previously developed strategies as well as over the current practice of moving vehicles to the nearest edge, the computation time for this formulation was about 2.5 times more than the formulation developed in [5]. So, a heuristic of cutting off the solver after a desired solution is obtained was developed and tested. The heuristic gave solutions that did not differ statistically from the optimal solutions and the differences between the paths suggested by the heuristic and the optimal solutions were minimal. This heuristic also gave a significant advantage of lower computation times and these results as well as computation times were practically usable and still provided improvement over the previously developed non-contraflow and current practice strategies.

Chapter two discusses the relevant work done in literature pertaining to the usage of contraflow in transportation and optimization models for providing paths to vehicles in autonomous systems. In chapter three, the requirements of the model as well as the preprocessing we perform on the inputs before running the optimization model has been described. Then, the mixed integer programming model is explained. Chapter four details the design of experiments to test sensitivity to problem parameters, computation times and comparison to current practice and the previously developed non-contraflow strategy from [6]. In chapter five, the analysis of the results is presented. In chapter six, the need for a heuristic is explained and the method and findings detailed. Finally, in chapter seven, conclusions have been drawn on the results found.

CHAPTER TWO

LITERATURE REVIEW

The utilization of the contraflow segment of the road to move more traffic is a common strategy used in evacuations [6, 7, 8, 9, 10]. Advantages as well as disadvantages of contraflow strategies exist. While the performance in terms of evacuation time improved, it is unavoidably associated with safety issues and challenges related to managing the flow of traffic at intersections when operating the contraflow. Plus, contraflow operations tend to be expensive affairs in terms of both labor and resources [6]. Reversing the direction of a lane in a smaller road with no raised median for a small section with no intersections, is however much easier and less expensive, resource and labor wise. This strategy is used in many cities when lanes are reversed on certain roads during rush hour [11]. However, in such situations also, the roads are primarily not designed for contraflow and this also causes confusion among drivers, which can lead to increased risk. These disadvantages apply to current systems where non-autonomous/ unconnected vehicles ply.

Autonomous vehicles offer new opportunities to utilize the contraflow segment additional labor and resources. When considering that we are dealing with autonomous or connected vehicles which receive precise instructions to travel, using an empty lane from the contraflow direction could be as simple as shifting a lane in regular traffic. Clearing a lane throughout the road link including exit ramps on freeways, intersections or at points where the traffic merges or separates, tends to reduce bottlenecks arising from using contraflow operations. This strategy allows for no vehicles moving in their usual direction in the contraflow lanes to travel in the reserved lanes, or even enter them, as the entry points are closed [10]. In another study, the reservation of a complete road has also been shown to increase the safety of travel of an emergency vehicle as well as improve its travel time [12]. This also makes sure that there are no head on collisions when using the contraflow. Next, we must ensure safety during entry and exit into the contraflow lane. It is important to ensure that we can accommodate the vehicles when we bring them back from the contraflow [10].

As discussed in the previous paragraph, lane reversal tends to be a laborious process which must be planned out carefully before hand. But, with advances in autonomous and connected vehicle systems, we can potentially direct the traffic towards any lane much more easily. In other words, the direction of travel in any lane of the road can be dynamically reversed at any given point in time. In the set of simulation experiments conducted in an autonomous vehicle environment, using dynamic lane reversal almost always improved the efficiency of traffic flow in the network [13]. This idea of utilizing an additional lane from the contraflow direction for a short distance gives rise to the question: Can we move the ERV into the contraflow for only a part of its travel so that it can move faster?

Optimization models are often used in vehicle path planning problems for varied objectives such as optimal fuel efficiency [14], shortest or fastest paths [11, 15]. Integer programming has been used to maximize fuel efficiency and/or travel time while routing multiple vehicles. A modified version of the maximum flow problem is also used to determine the direction of traffic movement on every lane of the road, indirectly using contraflow lanes when the traffic density is high or when there is considerable difference in traffic densities in the opposite directions of the roads [13]. There are several techniques used when trying to find the best route (time-wise or distance-wise) for a vehicle in an autonomous vehicle system. Markov decision processes are used to tackle stochasticity in traffic demand while determining the use of contraflow [16]. Also, due to complexity and the time sensitive nature of the dynamic lane reversal problem, heuristics are also used to reduce computation time [13,16].

The work described in this thesis is based on a similar idea, i.e., when the congestion differences are high, and the contraflow segment of the road is relatively empty, why not make use of the empty space to move the emergency vehicle into the contraflow lane to obtain faster speeds and reduced travel times?

The models also include strategies (constraints) to avoid collisions [11, 15]. We use a similar idea in our formulation to model the system such that there is no passing or weaving among the vehicles. Traffic simulation is another approach taken to iteratively find the fastest path along a link [15]. Certain guidelines such as clearing space in a lane or reserving a lane for an emergency vehicle in an autonomous/ connected vehicle environment have been developed in [17]. Strategies for safe and efficient maneuvers and lane shifts for an ERV in an automated vehicle system are introduced as well [18]. We utilize some of the strategies such as clearing the traffic in the lane before the ERV makes a move into the lane in our model as well.

The key to using contraflow strategies is to ensure safety of all vehicles on the road. We saw from previously cited literature that clearing a lane is one way to ensure safety [8].

However, since we discuss the task of creating an optimal path for the ERV to travel within a link, it is important to address the topic of safety regarding lane changes. To address this, we restrict a maximum of one lane change at a time for every vehicle, including the ERV, and we also restrict the ERV from entering the contraflow lane for a maximum of one time at every step (segment of the link). This is in line with previous work done on path planning in autonomous vehicle systems [16].

The results of the above described methods show that there is a significant improvement in the objective of the algorithm/ program, whether it is reduction in evacuation time, or speed of vehicles or fuel efficiency, when contraflow is used as an option. The literature discussed above also gives us evidence of the benefits of using optimization models for path planning in autonomous vehicle systems. There are also strategies in place to ensure safety of vehicular movement when contraflow is used. This encourages us to explore the contraflow strategy for optimizing ERV travel in an autonomous or connected vehicle system.

An integer linear program identifying the fastest ERV intra-link path is presented in [5]. This approach consists of (1) discretizing the road into a grid where all the cells have an identical size equal to the size of a vehicle plus buffer and (2) positioning each vehicle at a given cell in a way to free the fastest ERV path along the grid. In this thesis, this approach is extended and the ERV can switch to contraflow operations when needed and feasible. Conflicts between vehicles are reduced by introducing mathematical constraints [5]. The speed of the ERV is modeled as a discrete set of values, so the ERV can increase or decrease speed by one stage at a time. To further increase the safety of ERV travel, variables are defined to provide information about the space around the ERV in its path. When the ERV has relatively free surroundings, it can increase its speed whereas in dense vehicle environments around it, it needs to reduce or hold its speed [5]. We also include these environment variables into the objective and try to maximize the space around the ERV during its entire travel along the link, as it has been done in [5]. This work is an extension of the work done in [5] and we use the ideas presented there as a base to build a model for the contraflow lane as well. It is important to note that when operating on the contraflow lane, new safety implications exist as the ERV is now interacting with the vehicles travelling in the opposite direction. In this work, we have developed a revised and extended model to consider this issue as well.

Searches were conducted in databases on the utilization of contraflow strategies in transportation, contraflow usage in evacuations, lane reversal techniques, dynamic lane reversal and lane reversal in autonomous vehicle systems Searches were also made on path planning in autonomous vehicle systems and connected vehicle systems and motion control of vehicles in autonomous systems. Optimization models in vehicle routing and especially in intra-link vehicle routing were studied as well. Searches pertaining to research in emergency vehicle response time optimization were conducted as the work here describes particularly the optimization of ERV travel. Also, to understand the effects of ERV response times and provide motivation for our work, searches were conducted on reduction in emergency vehicle response times and the effects of response times of emergency services on mortality rates.

The databases that were searched include but are not limited to the transportation research board journals, ASCE transportation engineering journals, INFORMS journals on optimization, IEEE journals on autonomous systems and intelligent transportation systems.

CHAPTER THREE

MODEL DESCRIPTION

A road link is first divided into segments of predefined length (R_l) and each segment is modeled as a grid as shown in Figure 1. While this approach is similar to the model described in [5], there is one key change. While that model describes an initial range (IR) and an assignment range (AR) for the non-ERVs, in this thesis, the road segment is considered as one where the non-ERVs are currently moving and where they will be placed. This change allows for non-ERVs in the contraflow segment to be included in the road segment in consideration without separately defining an IR and AR for them. Also, since they are moving in the opposite direction, it is also not possible to specify exactly where the IR or AR starts. For this reason, the start and end of the contraflow segment are considered variables (explained later).

Each cell in the grid is C_l ft long ($C_l = 21$ for this thesis) and 1 lane or shoulder wide (Only shoulders which are wide enough to accommodate a vehicle are considered). The X-Y grid represents the original direction in which the ERV is traveling, while the X-Z grid represents the contraflow direction. The initial positions of all the non-ERVs (on both directions) as well as their initial speeds and braking capabilities are assumed to be known. Each non-ERV is shown as a small circle in Figure 1. Similarly, the initial lateral (Y dimension) position and the initial speed of the ERV are inputs to the model. The non-ERVs in the segment are numbered as shown in Figure 1 (vehicle number to the right of the vehicle) with one set of numbering for each direction. Consider the labeling from the perspective of the ERV, which would be located on the left in this figure. For both directions, the non-ERV labeling increases as we move away from the ERV in the x direction. If multiple vehicles occupy the same x position, the vehicle with a lower y or z coordinate is given the lower label number. The road composition is also known. A non-ERV on the rightmost lane of the original direction has an initial lateral (y) position of 2 if there is a shoulder and 1 if there is no shoulder. The presence of a median is considered as well in the model, with the inclusion of the contraflow parameter Ψ (detailed in the pre-processing section). The density of the vehicles for each direction of the road is analyzed to determine whether contraflow is allowed or not. Next, in a preprocessing step, the minimum stopping distance for each non-ERV is identified to define the range along the grid within which the non-ERV can stop (i.e. the optimization space). Subsequently, the formulation is run on this range as described in the following sections.

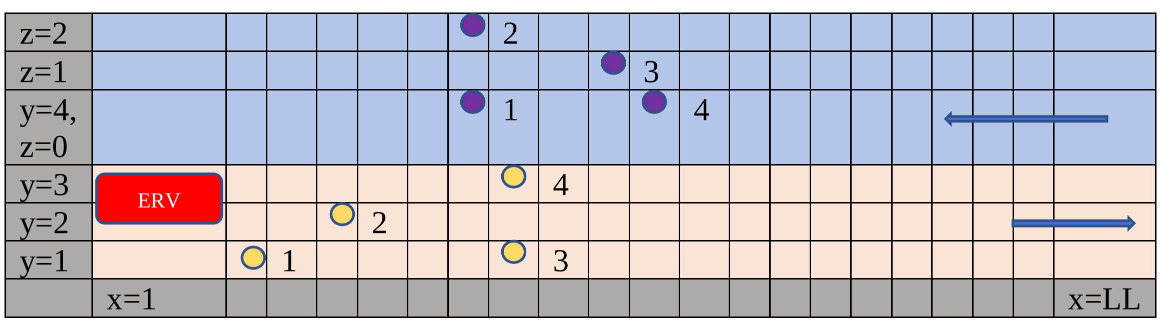

Figure 1: Model Description

3.1 Notation

Table 1 describes the parameters used in the mathematical model.

Table 1: Parameters

Notation	Meaning
λ_j	Minimum stopping distance in the equivalent of number of longitudinal cells for vehicle *j* in the normal direction
λ_k	Minimum stopping distance in the equivalent of number of longitudinal cells for vehicle *k* in contraflow direction
ω_j	Initial speed of vehicle *j* in normal direction in mph
ω_k	Initial speed of vehicle *k* in contraflow direction in mph
C_t	Approximate time needed to receive the vehicle data, compute the instructions to be sent and send the instructions to the vehicles in seconds (converted to hours for computation)
R_t	Approximate reaction time for the vehicles from the time that they are given the instructions in seconds (converted to hours for computation)
ξ_j	Comfortable deceleration rate of vehicle *j* in the normal direction in mph/h
ξ_k	Comfortable deceleration rate of vehicle *k* in the contraflow direction in mph/h

x'_j	Initial longitudinal position of vehicle *j* in normal direction
x'_k	Initial longitudinal position of vehicle *k* in contraflow
x''_j	Minimum final index for the vehicle *j* in normal direction according to its minimum stopping distance and its current longitudinal position on the road
x''_k	Minimum final index for the vehicle *k* in contraflow according to its minimum stopping distances and its current longitudinal position on the road
y'_j	Initial lateral position of vehicle *j* in normal direction
z'_k	Initial lateral position of vehicle *k* in contraflow direction
Y	Total number of lanes in the normal direction + 1, as we allow the ERV to travel in all the lanes of the original direction and the leftmost lane of the contraflow
Z	Total number of lanes in the contraflow direction – 1 as we added one additional lane from the contraflow the X-Y grid
N	ERV longitudinal size (in cells)

R_l	Length of the segment in consideration as number of cells
C_l	Length of every cell in the grid in ft.
I	Number of increments corresponding to the length of the segment and the ERV size = $\frac{R_l}{N+1} - 1$
c	The length (in number of cells) in which a non ERV can stop beyond its minimum final index
J	Number of vehicles in the road segment in the normal direction
K	Number of vehicles in the road segment in the contraflow
Ψ	Takes the value of 1 if the system allows contraflow and 0 otherwise
δ	Takes the value of 1 if there is no gap between the normal direction and contraflow lanes and 0 otherwise
s_{free}	Maximum speed the ERV can attain in the road segment
s_{min}	Minimum speed the ERV should maintain in the road segment

Table 2 describes the variables used in the mathematical model.

Table 2: Variables

$w^{x,y}$	Binary variable	Takes the value 1 if cell *(x,y)* is part of the ERV path and 0 otherwise Defined on *(x=1…R$_l$, y=1…Y)*
$v_j^{x,y}$	Binary variable	Takes the value 1 if non ERV *j* in the normal direction is assigned the cell *(x,y)* and 0 otherwise Defined on *(x=1…R$_l$, y=1…Y, j=1…J)*
$u_k^{x,z}$	Binary variable	Takes the value 1 if non ERV *k* in the contraflow direction is assigned the position *(x,z)* and 0 otherwise Defined on *(x=1…R$_l$, z=1…Z, k=1…K)*
φ_k	Binary Variable	Takes the value 1 if non ERV *k* in the opposing direction is going to be assigned a position from the formulation and 0 otherwise Defined on *(k=1…K)*
φ'_k	Binary Variable	Takes the value of 1 if the minimum final index of vehicle *k* in the contraflow direction falls behind the starting point of contraflow and 0 otherwise

		Defined on *(k=1…K)*
φ''_k	Binary Variable	Takes the value of 1 if the final potential location of the vehicle *k* in the contraflow direction falls in front of the ending point of contraflow and 0 otherwise Defined on *(k=1…K)*
α	Integer variable	Starting longitudinal position (along the link with respect to the start of the link segment) of the contraflow in which non-ERVs in the contraflow are being assigned positions and the ERV might move in the contraflow from here
β	Integer variable	Ending longitudinal position (along the link with respect to the start of the link segment) of the contraflow in which non-ERVs in the contraflow are being assigned positions and the ERV goes back to the normal direction
τ	Integer variable	Size of the contraflow segment where the ERV might move as number of cells

$d_1^{i,y}$	Binary Variable	Takes the value of 1 if the direction given to the ERV at the increment *i* is "right" at lateral position *y* and 0 otherwise Defined on *(i=1…I, y=1…Y)*
$d_2^{i,y}$	Binary Variable	Takes the value of 1 if the direction given to the ERV at the increment *i* is "straight" at lateral position *y* and 0 otherwise Defined on *(i=1…I, y=1…Y)*
$d_3^{i,y}$	Binary Variable	Takes the value of 1 if the direction given to the ERV at the increment *i* is "left" at lateral position *y* and 0 otherwise Defined on *(i=1…I, y=1…Y)*
s^i	Integer variable	ERV actual speed at the increment *I* Defined on *(i=1…I)*
s_{env}^i	Integer variable	ERV speed as determined by the presence of vehicles around it at increment *i* Defined on *(i=1…I)*

s_{temp}^{i}	Integer variable	Temporary speed variable for the ERV at increment *i* Defined on *(i=1…I)*
ϑ_{temp}^{i+1}	Binary variable	Takes the value of 1 if $s_{temp}^{i} \geq s_{min}$ and 0 otherwise Defined on *(i=1…I-1)*

3.2 Pre-processing

Each vehicle travelling at a defined speed (ω_j) requires a minimum distance to reach a complete stop, which is the distance travelled during the computation time C_t and the reaction time R_t. Hence, the minimum stopping distance (λ_j and λ_k) of each non-ERV j and non-ERV k is calculated using equation 1 [5] (for vehicles in the normal direction) and equation 3 (for vehicles in the contraflow direction) respectively. The minimum stopping distance depends on the vehicle's braking capacity (ξ_j, ξ_k), initial speed (ω_j, ω_k), the computation and reaction times(C_t, R_t). The vehicle can travel more distance also, based on how much it brakes. The equations give the minimum distance needed. The factor C_l is added to convert the minimum stopping distance from ft to number of cells.

Equation 2 [5] computes the minimum final position for vehicles in the normal direction. It is the sum of the minimum stopping distance (in terms of cells) and the initial longitudinal (x) position of the vehicle j as it travels in the direction of increasing x coordinates in the grid.

$$\lambda_j = ceil((\omega_j(C_t + R_t) + 0.5\frac{{\omega_j}^2}{\xi_j})/C_l)\ \ \forall j = 1 \dots J \quad (1)$$

$$x"_j = x'_j +\ minstp_j\ \ \forall j = 1 \dots J \quad (2)$$

Equation 4 computes the minimum final position for vehicles in the contraflow direction. The minimum stopping distance is subtracted from the initial position as the vehicle travels in the direction opposite to the increasing x-coordinates in the grid.

$$\lambda_k = floor((\omega_k(C_t + R_t) + 0.5\frac{{\omega_k}^2}{\xi_k})/C_l)\ \ \forall k = 1 \dots K \quad (3)$$

$$x"_k = x'_k -\ minstp_k\ \ \forall k = 1 \dots K \quad (4)$$

The preprocessing identifies the vehicles which can potentially stop outside the road segment under consideration, so that they are excluded from the formulation. For example, if a non- ERV is moving in the normal direction, currently near the end of the segment, and its minimum stopping position is outside the segment under consideration, it is instructed to stop outside of the segment and not included in the formulation.

Another pre-processing step determines whether usage of contraflow by the ERV is a viable option. The use of contraflow is not permitted when the traffic density is low on the normal direction, or if the traffic density on the contraflow direction is higher than that on the normal direction. The presence of a median between directions implies no contraflow. A parameter $\boldsymbol{\Psi}$ takes the value of 1 when contraflow can occur (i.e., if all the following conditions apply) and 0 otherwise:

- If the traffic density in the normal direction is greater than a certain threshold (v/c=0.5 for this thesis);
- If the traffic density difference between the normal and contraflow directions is greater than a certain threshold (v/c difference=0.1 for this thesis); and
- No median

In this work, a single switch from contraflow and back to normal direction is allowed per segment when Ψ is 1.

3.3 Formulation

The following section describes the mixed integer programming formulation in detail along with every constraint and the objective function.

3.3.1 Constraints

Equation 5 [5] ensures (1) that the ERV can only travel along the normal direction's lanes and along the leftmost lane of the contraflow direction and (2) that the ERV is assigned to only one cell at each position (x).

$$\sum_{y=1}^{Y} w^{x,y} = 1 \ \forall x = 1 \dots R_l \tag{5}$$

At most one vehicle may occupy any cell. Equation 6 [5] applies for vehicles in the normal direction while Equation 7 ensures the same condition holds for the lanes in the opposing direction.

$$w^{x,y} + \sum_{j=1}^{J} v_j^{x,y} \leq 1 \ \forall x = 1 \dots R_l; \forall y = 1 \dots Y \quad (6)$$

$$\sum_{k=1}^{K} u_k^{x,z} \leq 1 \ \forall x = 1 \dots R_l; \ z = 1 \dots Z \quad (7)$$

The feasible stopping range (FSR) of each non-ERV is identified (i.e., limited range along the link where the non-ERV can stop). The FSR of vehicle j starts at the minimum final position of j (x''_j) and extends 'c' cells beyond that (i.e., to reduce vehicle interactions, the FSR size is limited to 'c' cells). Equation 8 [5] ensures that each non-ERV initially travelling in the normal direction is assigned to a cell along its corresponding FSR.

In the opposing direction, only non-ERVs that are included in the optimization problem (i.e., whose minimum final position falls between the start and end of the contraflow range) are assigned to a cell in their corresponding FSRs on the opposing direction (Constraints identifying when the non-ERVs in the opposing direction are considered are explained below). Equation 10 specifies the range for the non-ERV in the contraflow to stop in (be assigned final position), if it is being considered. Otherwise, the vehicle is not assigned a position. If the vehicle is being assigned a position, it is not allowed to stop in the left-most lane of the contraflow.

Each non-ERV is given only a single position in the entire grid. Equations 9 [6] and 11 ensure that every non-ERV is assigned to only one cell in its corresponding direction.

$$\sum_{x=x"_j}^{x"_j+c} \sum_{y=1}^{Y-1} v_j^{x,y} = 1 \ \forall j = 1 \dots J \tag{8}$$

$$\sum_{x=1}^{LL} \sum_{y=1}^{Y} v_j^{x,y} = 1 \ \forall j = 1 \dots J \tag{9}$$

$$\sum_{x=x"_k}^{x"_k-c} \sum_{z=1}^{Z} u_k^{x,y} = \varphi_k \ \forall k = 1 \dots K \tag{10}$$

$$\sum_{x=1}^{LL} \sum_{z=1}^{Z} u_k^{x,y} = \varphi_k \ \forall k \dots K \tag{11}$$

To identify whether a non-ERV in the opposing direction should be assigned a position or not, the start and end of the contraflow in which the ERV will travel has to be identified. Equation 12 defines the start of the contraflow as the point at which the ERV makes a lane change into the left most lane of the contraflow. Equation 13 defines the length of the contraflow region as the total of number of cells traveled by the ERV in the contraflow plus a buffer equal to the length of one ERV needed by the ERV to maneuver back to the normal direction. Equation 14 gives the position corresponding to the end of the contraflow as a function of the starting point and the length of the contraflow being considered. Fixing the start and end of the contraflow segment as the same as the start and end of the road segment in consideration respectively is unnecessary as there is a chance that the ERV may never make a move into the contraflow yet, the vehicles would be assigned positions. By making them variables, we give freedom to the optimization model to decide if the optimal solution requires positions given to the non-ERVs in contraflow.

$$\alpha = 1 + \sum_{i=1}^{I} i * (N+1) * d_3^{i,Y-1} \tag{12}$$

$$\tau = \sum_{x=1}^{R_l} w^{x,Y} + N \tag{13}$$

$$\beta = \alpha + \tau - 1 \tag{14}$$

Equations 15 and 16 determine if a non-ERV in the contraflow has a stopping position corresponding to its minimum stopping distance that has a x-coordinate greater than the point at which the ERV enters contraflow. Equations 17 and 18 determine if the non-ERV in the contraflow has a stopping position corresponding to its minimum stopping distance that has a x-coordinate less than the point at which the ERV exits the contraflow. Equations 19 and 20 ensure that if equations 15-18 are satisfied for a non-ERV, then it is considered in the contraflow range and assigned a position.

$$x_k^{"} \geq \alpha - R_l * \left(1 - \varphi'_k\right) \;\; \forall k = 1 \ldots K \tag{15}$$

$$\alpha \geq x_k^{"} - R_l * \varphi'_k \;\; \forall k = 1 \ldots K \tag{16}$$

$$\beta \geq x_k^{"} - R_l * (1 - \varphi"_k) \;\; \forall k = 1 \ldots K \tag{17}$$

$$x_k^{"} \geq \beta - R_l * \varphi"_k \;\; \forall k = 1 \ldots K \tag{18}$$

$$\varphi_k \leq \frac{\varphi'_k + \varphi"_k}{2} \;\; \forall k = 1 \ldots K \tag{19}$$

$$\varphi_k \geq \left(\varphi'_k + \varphi"_k\right) - 1 \;\; \forall k = 1 \ldots K \tag{20}$$

Equation 21 ensures that the ERV can make a left lane change into the contraflow only when Ψ is equal to 1.

$$\sum_{i=1}^{I} d_3^{i,(Y-1)} \leq \Psi \tag{21}$$

Equation 22 ensures that the ERV shifts back to the normal direction before the end of the link segment, in cases when it has entered the contraflow. The shift must occur at least one increment before the end of the segment.

$$\sum_{i=1}^{I} d_1^{i,Y} = \sum_{i=1}^{I} d_3^{i,Y-1} \tag{22}$$

For safety concerns, we do not allow passing among non-ERVs in both directions. Equation 23 ensures that if a non-ERV *j'* in the normal direction is initially ahead of *j*, then, even in the final assignment, *j'* must be ahead of *j* or at least in the same lateral position as *j*. Equation 24 ensures the same condition is satisfied for the contraflow vehicles as well. However, in the contraflow, these constraints are binding only if both vehicles are considered in the formulation.

This idea is carried over from [5] but this mathematical constraint is newly modeled. The constraints in [5] could not safely ensure the no passing/weaving constraint in one type of situation: When a sample non-ERV 1 had a minimum stopping position less than another non-ERV 2, and its initial lateral position also less than the lateral position of non-ERV 2, then there was a chance that the two non-ERVs could still cross each other's paths without violating any of the constraints. Now, since in such cases, the non-ERVs might still not conflict as they might not be at the crossing point at the same point in time, there is still a chance of conflict. The newly modeled constraints eliminate the chance of an intersection of paths among non-ERVs, hence, providing additional safety.

The formulation in [5] uses the big-M method of formulating many constraints. While this approach is easy to understand and model, it is not computationally efficient. So, if bounds can be found on the variables without using a big-M, the constraints have been formulated with such bounds wherever possible. The constraints which use the big-M in [5] have been remodeled with relevant bounds as well. For example, in Equation 24 below, the term R_l gives a bound on the term on the left-hand side (LHS) of the inequality and hence has been used instead of the big-M.

$$\sum_{x=1}^{R_l}\sum_{y=1}^{Y-1} x * v_j^{x,y} \leq \sum_{x=1}^{R_l}\sum_{y=1}^{Y-1} x * v_{j'}^{x,y} \;\; \forall j' > j \tag{23}$$

$$\sum_{x=1}^{R_l}\sum_{z=1}^{Z} x * u_k^{x,y} \leq \sum_{x=1}^{R_l}\sum_{z=1}^{Z-1} x * u_{k'}^{x,y} + R_l * (2 - \varphi_k - \varphi_{k'}) \;\; \forall k' > k \tag{24}$$

Similarly, weaving among non-ERVs is prohibited in both directions. Equation 25 ensures that a non-ERV *j'* which is to the left of j in the normal direction initially, is always placed left of *j* or in the same x position in the final assignment also. Equation 26 ensures the same condition when a vehicle *j'* is to the right of *j*. Equation 27 and 28 ensure the same conditions are obeyed by the contraflow vehicle assignments if both vehicles are considered.

In Equations 27 and 28, Z gives an upper bound on the LHS and hence has been used instead of the big-M.

$$\sum_{x=1}^{R_l}\sum_{y=1}^{Y-1} y * v_j^{x,y} \leq \sum_{x=1}^{R_l}\sum_{y=1}^{Y-1} y * v_{j'}^{x,y} \ \ \forall j' > j \ \ni y'_j \leq y'_{j'} \tag{25}$$

$$\sum_{x=1}^{R_l}\sum_{y=1}^{Y-1} y * v_j^{x,y} \geq \sum_{x=1}^{R_l}\sum_{y=1}^{Y-1} y * v_{j'}^{x,y} \ \ \forall j' > j \ \ni y'_j \geq y'_{j'} \tag{26}$$

$$\sum_{x=1}^{R_l}\sum_{z=1}^{Z} z * u_k^{x,y} \leq \sum_{x=1}^{R_l}\sum_{z=1}^{Z-1} z * u_{k'}^{x,y} + Z * (2 - \varphi_k - \varphi_{k'}) \ \ \forall k' > k \ \ni y'_k \leq y'_{k'} \tag{27}$$

$$\sum_{x=1}^{R_l}\sum_{z=1}^{Z} z * u_k^{x,y} \geq \sum_{x=1}^{R_l}\sum_{z=1}^{Z-1} z * u_{k'}^{x,y} + Z * (2 - \varphi_k - \varphi_{k'}) \ \ \forall k' > k \ \ni y'_k \geq y'_{k'} \tag{28}$$

Equation 29 [5] ensures that only one set of instructions is given to the ERV at each increment.

$$\sum_{y=1}^{Y}\sum_{q=1}^{3} d_q^{i,y} = 1; \ \ \forall\ i = 1 \dots I \tag{29}$$

Equations 30 and 31 [5] imply that the ERV cannot move to another lane if there is no space to move, that is, it cannot move right at the rightmost lane or move left at the contraflow lane.

$$d_1^{i,1} = 0 \ \ \forall i = 1 \dots I \tag{30}$$

$$d_3^{i,Y} = 0 \ \ \forall i \tag{31}$$

Equations 32-33 [5] say that the ERV can make a right lane shift if the ERV is assigned a position in its current lane and enough cells (depending on the size of the ERV) in the lane to the right of its current lane. Equations 34-35 [5] say the ERV can stay on the same lane for the next increment if it is assigned a position in same lane for $N + 1$ cells ahead of it and its current cell. Equations 36-37 [5] enforce the same condition when it makes a left lane shift. This set of equations provides a link between the ERV position variables and the direction instruction variables.

$$d_1^{i,y} \leq \frac{w^{i(N+1),y} + w^{i(N+1)+t,y-1}}{2} \quad \forall i = 1 \dots I;\ \forall t = 1 \dots N+1;\ \forall y = 2 \dots Y \tag{32}$$

$$d_1^{i,y} \geq w^{i(N+1),y} + w^{i(N+1)+t,y-1} - 1 \quad \forall i = 1 \dots I;\ \forall t = 1 \dots N+1;\ \forall y = 2 \dots Y \tag{33}$$

$$d_2^{i,y} \leq \frac{w^{i(N+1),y} + w^{i(N+1)+t,y}}{2} \quad \forall i = 1 \dots I;\ \forall t = 1 \dots N+1;\ \forall y = 1 \dots Y \tag{34}$$

$$d_2^{i,y} \geq w^{i(N+1),y} + w^{i(N+1)+t,y} - 1 \quad \forall i = 1 \dots I;\ \forall t = 1 \dots N+1;\ \forall y = 1 \dots Y \tag{35}$$

$$d_3^{i,y} \leq \frac{w^{i(N+1),y} + w^{i(N+1)+t,y+1}}{2} \quad \forall i = 1 \dots I;\ \forall t = 1 \dots N+1;\ \forall y = 1 \dots Y-1 \tag{36}$$

$$d_3^{i,y} \geq w^{i(N+1),y} + w^{i(N+1)+t,y+1} - 1 \quad \forall i = 1 \dots I;\ \forall t = 1 \dots N+1;\ \forall y = 1 \dots Y-1 \tag{37}$$

Equation 38 ensures that when the ERV goes straight, there are no non-ERVs in its path in the next increment. Equations 39-40 ensure the same condition when the ERV makes a right lane change, but also empties more cells around the path of the ERV for better safety during lane change. Equations 41-42 ensure the same condition when the ERV makes a left lane change. These equations have been remodeled from [5] to include appropriate bounds on the LHS and replacing the big-Ms for better computational efficiency.

$$\sum_{x=t'}^{T'}\sum_{j=1}^{J} v_j^{x,y} \leq (N+1) * \left(1 - d_2^{i,y}\right)\ \forall y = 1 \dots Y-1;\ \forall i = 1 \dots I \tag{38}$$

$where\ t' = (N+1)i + 1;\ T' = (N+1)i + (N+1)$

$$\sum_{x=t'}^{T''}\sum_{j=1}^{J} v_j^{x,y} + \sum_{x=t'}^{T'}\sum_{j=1}^{J} v_j^{x,y-1} \leq (2N+1) * \left(1 - d_1^{i,y}\right);\ \forall y = 2 \dots Y-1;\ \forall i = 1 \dots I \tag{39}$$

$where\ t' = (N+1)i + 1;\ T' = (N+1)i + (N+1);\ T'' = (N+1)i + N$

$$\sum_{x=t'}^{T'}\sum_{j=1}^{J} v_j^{x,Y-1} \leq (N+1) * \left(1 - d_1^{i,Y}\right);\ \ \forall i = 1 \dots I \tag{40}$$

$where\ t' = (N+1)i + 1;\ T' = (N+1)i + (N+1)$

$$\sum_{x=t'}^{T''}\sum_{j=1}^{J} v_j^{x,y} + \sum_{x=t'}^{T'}\sum_{j=1}^{J} v_j^{x,y+1} \leq (2N+1) * \left(1 - d_3^{i,y}\right);\ \forall y = 1 \dots Y-2;\ 1 \dots I \tag{41}$$

$where\ t' = (N+1)i + 1;\ \ T' = (N+1)i + (N+1);\ T'' = (N+1)i + N$

$$\sum_{x=t'}^{T''}\sum_{j=1}^{J} v_j^{x,Y-1} \leq (N+1) * \left(1 - d_3^{i,Y-1}\right);\ \forall i = 1 \dots I \tag{42}$$

$where\ t' = (N+1)i + 1;\ \ T'' = (N+1)i + N$

The ERV speed depends on the surrounding vehicles, ERV instructions and speed limits. Also, since this is a discrete optimization model, the speed of the ERV has been discretized into speed stages where each speed stage represents a specific speed. The speed stage table can be requested if needed.

Equation 43 indicates that if the ERV is traveling in one of the middle lanes of the normal direction, then the environmental speed variable can increase by 1 if there are no non-ERVs on both the right and left adjacent lanes to the lane of the ERV. If for example, the ERV is moving straight in the second lane, then its environment speed variable can increase by 1 if the first and third lanes are empty. Equation 44 enforces the same condition for the last increment.

Equations 43-49 have also been remodeled by replacing the big-Ms by bounds of maximum attainable speeds.

$$s_{env}^{i+1} = s^i + 1 - \sum_{j=1}^{J} v_j^{(N+1)i+t,y-1} - \sum_{j=1}^{J} v_j^{(N+1)i+t,y+1} + s_{free} * \left(1 - w^{(N+1)i+t,y}\right) \tag{43}$$

$\forall i = 1 \dots I-1\,; \forall t = 0 \dots N+2;\ \forall y = 2 \dots Y-2$

$$s_{env}^{LL/(N+1)} \leq s^{\frac{LL}{N+1}-1} + 1 - \sum_{j=1}^{J} v_j^{LL-(N+1)+t,y-1} - \sum_{j=1}^{J} v_j^{LL-(N+1)+t,y+1} + s_{free} * \left(1 - w^{LL-(N+1)+t,y}\right. \tag{44}$$

$\forall t = 0 \dots N+1; \forall y = 2 \dots\ Y-2$

If the ERV is in the rightmost lane, it can increase its speed by 1 if there are no vehicles in the adjacent lane. Otherwise, its speed remains the same. This condition is enforced by equations 45-46 where 46 enforces the condition for the last increment.

$$s_{env}^{i+1} \leq s^i + 1 - \sum_{j=1}^{J} v_j^{(N+1)i+t,2} + s_{free} * \left(1 - w^{(N+1)i+t,1}\right); \tag{45}$$

$\forall i = 1 \dots I-1\,; \forall t = 0 \dots N+2$

$$s_{env}^{LL/(N+1)} \leq s^{\frac{LL}{N+1}-1} + 1 - \sum_{j=1}^{J} v_j^{LL-(N+1)+t,2} + s_{free} * \left(1 - w^{LL-(N+1)+t,1}\right) \tag{46}$$

$\forall t = 0 \ldots N + 1$

When the ERV is in the leftmost lane of the normal direction, the environmental speed variable is constrained by the same rule by the vehicles in the adjacent right lane. Equations 47-48 ensure this constraint where 48 is for the last increment.

$$s_{env}^{i+1} \leq s^{i} + 1 - \sum_{j=1}^{J} v_j^{(N+1)i+t,Y-2} + s_{free} * \left(1 - w^{(N+1)i+t,Y-1}\right); \tag{47}$$

$\forall i = 1 \ldots I - 1 \,; \forall t = 0 \ldots N + 2$

$$s_{env}^{LL/(N+1)} \leq s^{LL/(N+1)-1} + 1 - \sum_{j=1}^{J} v_j^{LL-(N+1)+t,Y-2} + s_{free}\left(1 - w^{LL-(N+1)+t,Y-1}\right); \tag{48}$$

$\forall t = 0 \ldots N + 1$

When the ERV is in the contraflow lane, it can increase its speed by 1 if the opposing traffic lane next to it is free and if the adjacent lane to the right of it is free. However, the speed of the ERV when it is in the contraflow lane is not constrained by the presence of vehicles in the normal direction if there is a gap (not a median) in the road between the normal and contraflow sections of the road ($\delta = 0$). Equation 49 ensures the above condition.

$$s_{env}^{i+1} \leq s^{i} + 1 - \left(\sum_{k} u_{k}^{(N+1)i+t,1}\right) - \delta * (\sum_{j} v_{j}^{(N+1)i+t,Y-1}) + s_{free}\left(1 - w^{(N+1)i+t,Y}\right) \quad (49)$$

$$\forall i = 1 \ldots I - 1, \forall t = 0 \ldots N + 2$$

The speed of the ERV is restricted by the surrounding non-ERVs as well as by the lane changes of the ERV itself and the speed limit. First, a temporary variable is defined to enforce the environment and lane change restrictions on the speed of the ERV. Equation 50 ensures that the temporary speed variable is limited to the environment speed variable. Equation 51 links it to the lane shift constraints on the speed of the ERV. Equations 52 and 53 limit the speed of the ERV. Equations 54-55 link the speed of the ERV to the temporary speed variable. Equation 56 ensures that the speed reductions recommended due to lane changes and environment restrictions are ignored when the ERV is at minimum speed [5], that is, the ERV speed does not drop below the minimum speed.

$$s_{temp}^{i+1} \leq s_{env}^{i+1}; \quad \forall\, i = 1 \ldots I \quad (50)$$

$$s_{temp}^{i+1} \leq s^{i} + 2\sum_{y=1}^{Y} d_{2}^{i,y} - 1; \quad \forall\, i = 1 \ldots I \quad (51)$$

$$s^{i+1} \leq s_{free}; \quad \forall\, i = 1, \ldots, LL/(N+1) - 1 \quad (52)$$

$$\mathrm{s}^{\mathrm{i+1}} \geq \mathrm{s}_{\mathrm{min}}\,; \ \forall\, \mathrm{i} = 1 \ldots \mathrm{I} \quad (53)$$

$$\mathrm{s}^{\mathrm{i+1}} \geq \mathrm{s}_{\mathrm{temp}}^{\mathrm{i+1}}; \forall\, \mathrm{i} = 1 \ldots \mathrm{I} \quad (54)$$

$$\mathrm{s}^{\mathrm{i+1}} \leq \mathrm{s}_{\mathrm{free}} * \left(1 - \vartheta_{\mathrm{temp}}^{\mathrm{i+1}}\right) + \mathrm{s}_{\mathrm{temp}}^{\mathrm{i+1}}; \quad \forall\, \mathrm{i} = 1 \ldots \mathrm{I} \quad (55)$$

$$\mathrm{s}^{\mathrm{i+1}} \leq \mathrm{s}_{\mathrm{free}} * \vartheta_{\mathrm{temp}}^{\mathrm{i+1}} + \mathrm{s}_{\mathrm{min}}; \quad \forall\, \mathrm{i} = 1 \ldots \mathrm{I} \quad (56)$$

3.3.2 Objective

The objective is to maximize the ERV's speed while encouraging safety by moving the non-ERVs away from the ERV's path through the environment speed variable [5].

$$\mathrm{Max}\,Z = \sum_{i=2}^{LL/(N+1)} s^i + \sum_{i=2}^{LL/(N+1)} s_{env}^i \tag{57}$$

CHAPTER FOUR

NUMERICAL EXPERIMENTS

The experimental analysis includes the following tests: (1) sensitivity to initial parameters and computation time studies, (2) comparison with the non-contraflow scenario, and (3) comparison with the current practice of moving vehicles to the nearest edge. The tests were conducted using the NEOS Server with CPLEX Solver.

4.1 Stage 1: Sensitivity analysis and computation time studies

The first stage of the experimental analysis is conducted to find the characteristics of the optimal paths and ERV speed variations when the initial problem parameters are varied. Also, the effect of the problem parameters on computation time has been analyzed.

- Type of ERV: Ambulance or police vehicle.
- Type of road: Arterial, major and minor collectors.
- The initial speed of the ERV.
- The initial lateral position (lane) of the ERV.
- The traffic congestion on each direction of the road segment.
    - The traffic congestion is expressed in terms of the volume to capacity ratio and then converted to the corresponding number of vehicles from the data in [19].
- Length of the road segment (R_l).
- Length of feasible stopping range (c).
- Assumptions

- No median in the road segment
- The environment of the ERV is not affected by vehicles in the normal direction when it is moving in the contraflow segment, that is, there is a gap in the road segment between the two sides ($\delta = 0$).
- Non-ERV speeds and deceleration capabilities (fixed at 25000 mph/h) are homogenous.

The set of experiments conducted are listed in Tables 3 and 4. Table 4 shows the parameters that are fixed for the tests in which the length of the road segment has been varied.

Table 3: Experiments for sensitivity and computation time analysis

ERV type	Road type	ERV initial speed	ERV initial position	Road composition	V/C ratio - original direction	V/C ratio - contraflow	NonERV speed (mph)	length (number of cells)	Total vehicles per mile per lane normal	Total vehicles per mile per lane contraflow	Total number of vehicles normal	Total number of vehicles contraflow
Ambulance	Arterial	8	5	4 lanes 1 shoulder	0.6	0.4	40	48	22	13	18	11
		8	4		0.6	0.4			22	13	18	11
		6	5		0.8	0.6			30	22	24	18
		6	4		0.8	0.6			30	22	24	18
		6	5		0.8	0.4			30	13	24	11
		6	4		0.8	0.4			30	13	24	11
	Major Collector	4	4	3 lanes 1 shoulder	0.6	0.4	30		22	13	13	8
		4	3		0.6	0.4			22	13	13	8
		3	4		0.8	0.6			30	22	18	13
		3	3		0.8	0.6			30	22	18	13
		3	4		0.8	0.4			30	13	18	8
		3	3		0.8	0.4			30	13	18	8
	Minor Collector	3	3	2 lanes 1 shoulder	0.6	0.4	20		22	13	9	6
		3	2		0.6	0.4			22	13	9	6
		2	3		0.8	0.6			30	22	12	9
		2	2		0.8	0.6			30	22	12	9
		2	3		0.8	0.4			30	13	12	6
		2	2		0.8	0.4			30	13	12	6
Police	Arterial	6	5	4 lanes 1 shoulder	0.6	0.4	40		22	13	18	11
		6	4		0.6	0.4			22	13	18	11
		5	5		0.8	0.6			30	22	24	18
		5	4		0.8	0.6			30	22	24	18
		5	5		0.8	0.4			30	13	24	11
		5	4		0.8	0.4			30	13	24	11
	Major Collector	3	4	3 lanes 1 shoulder	0.6	0.4	30		22	13	13	8
		3	3		0.6	0.4			22	13	13	8
		2	4		0.8	0.6			30	22	18	13
		2	2		0.8	0.6			30	22	18	13
		2	4		0.8	0.4			30	13	18	8
		2	2		0.8	0.4			30	13	18	8
	Minor Collector	3	3	2 lanes 1 shoulder	0.6	0.4	20		22	13	9	6
		3	2		0.6	0.4			22	13	9	6
		2	3		0.8	0.6			30	22	12	9
		2	2		0.8	0.6			30	22	12	9
		2	3		0.8	0.4			30	13	12	6
		2	2		0.8	0.4			30	13	12	6

Table 4: Experiments for length of road segment tests

Parameter	**Value**
ERV initial position	2 (y=3)
Type of road	Collector (3 lanes, 1 shoulder)
Type of ERV	Ambulance
Initial speed of ERV	4

v/c ratio of original direction	0.6
v/c ratio of contraflow	0.4
Homogenous non-ERV speed	25 mph
Feasible stopping range length	5 cells
ERV initial speed and lateral position	Speed stage 6 and leftmost lane of normal direction
Length of road segment*	Varied from 0.05 to 0.3 mile in steps of 0.05
Feasible stopping range*	Varied from 2 to 13 cells

*correspond to the tests of change in road segment length or FSR size

4.2 Stage 2: Comparison to non-contraflow strategy

In this experiment, comparison studies were conducted on the formulation to the same cases in Table 3 with and without the contraflow option enabled, and the computation times, average speeds of the ERV and travel times were recorded and analyzed.

4.3 Stage 3: Comparison to current practice

In stage 3, constraints were added to every non-ERV to move to the nearest edge. For example, in a 5-lane road, a non-ERV on the 4th lane was instructed to move to the 5th lane. Then, the extended formulation was solved and compared to the scenario when the constraints were removed, and contraflow was enabled. The results were analyzed for travel times and average speeds of the ERV through the segment.

CHAPTER FIVE

RESULTS

5.1 Description of a sample result

Figure 2 gives a sample road picture which will be used throughout this section as a template for every road picture shown. The red-black line corresponds to the path of the ERV along the road. The other colored lines represent the non-ERVs moving from their starting positions to their ending positions. Note that the normal direction lanes are shown on the negative Y-axis and the contraflow lanes shown on the non-negative Y-axis. The X-axis corresponds to the cell-number on the grid. The caption is explained as [type of road – type of ERV – ERV starting lane position – v/c ratio of normal direction – v/c ratio of contraflow direction].

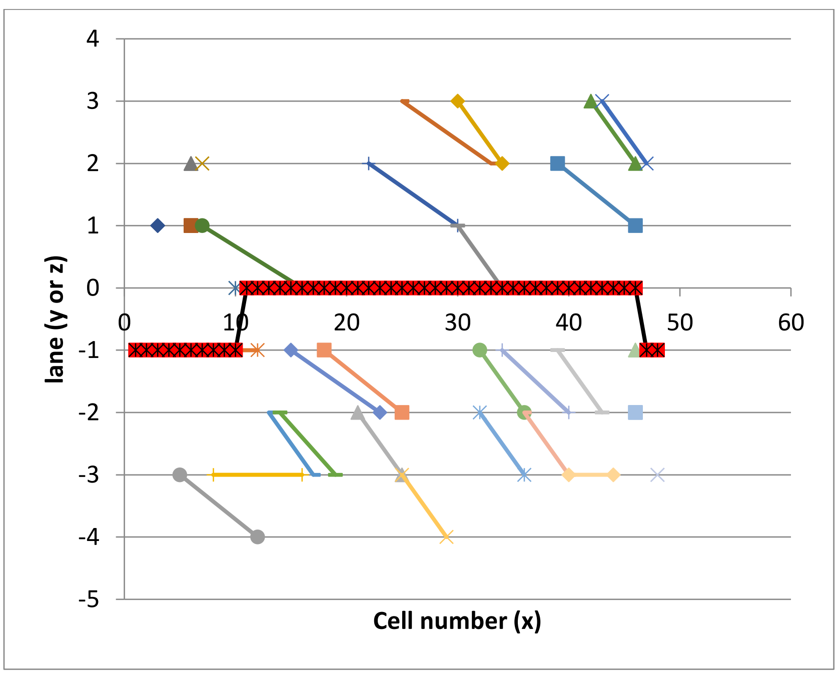

Figure 2: Sample road picture – Major – Ambulance – left – 0.8 – 0.6

5.2 Sensitivity analysis and computation time studies

5.2.1 Initial position of the ERV

The initial position of the ERV is a major factor in determining the usage of contraflow. When the ERV starts from the leftmost lane of the normal direction, the optimal path almost always includes a shift into the contraflow as observed in sample figures 3a and 4a. This trend is also observed in figures 21a, 23a, 25a, 29a, 31a, 35a, 37a, 39a, 43a, 45a, 47a, 49a and 53a in the appendix. The contraflow option offers a significant improvement since the number of lane shifts is only 1 and since contraflow is considered a viable option only when its density is less than the normal direction traffic. When the ERV starts in the leftmost lane, it makes a shift to the contraflow and the speed increase is rapid in such situations as observed in sample figures 3b, 4b and in figures 21b, 23b, 25b, 29b, 31b, 35b, 37b, 39b, 43b, 45b, 47b, 49b and 53b in the appendix. When the ERV starts in a middle lane, it does not make a shift into the contraflow as often as when it starts from the leftmost lane. This trend is seen in sample cases 6a and 6b and in figures 22a, 24a, 26a, 28a, 34a, 36a, 38a, 40a, 42a, 44a, 50a, 52a, 54a and 56a in the appendix. This is because of the loss in speed when it has made more than one lane change. But, in some cases as seen in figures 7a and 7b, the ERV moves to the contraflow lane even when it starts on the middle or the rightmost lane. This trend is also observed in figures 30a, 32a, 46a and 48a in the appendix. This output was only obtained when dealing with police vehicle (more maneuvers to make in the road segment due to the reduced ERV size). Since it was observed that small ERVs make more maneuvers in the same segment length, it can be concluded that larger ERVs too can make more maneuvers and hence use the contraflow option more often in larger segments as seen in a sample instance shown in figure 5 where the length of the segment was 0.6 mile and the congestion was very high (v/c = 1) in the normal direction and the contraflow was less congested (v/c = 0.1). When the ERV starts from the leftmost lane, the computation time required to obtain the optimal solution is also less than when the ERV starts in the middle lane as observed in graphs 8a-b. This may be due to the solver finding the best solution quickly by using the contraflow. The average speeds are slightly higher (1 mph on average) when the ERV starts in the leftmost lane.

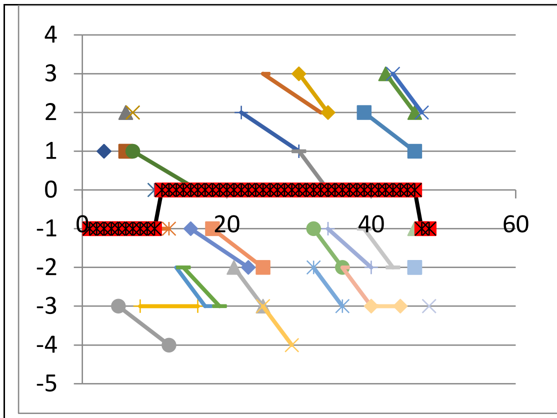

Figure 3a: sample road picture – Major – Ambulance – left - 0.8 – 0.6

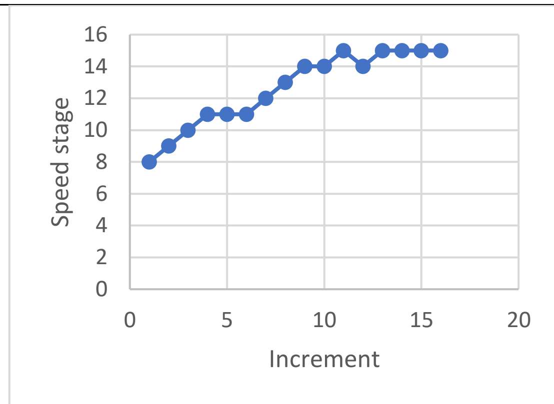

Figure 3b: Speed stage vs Increment plot

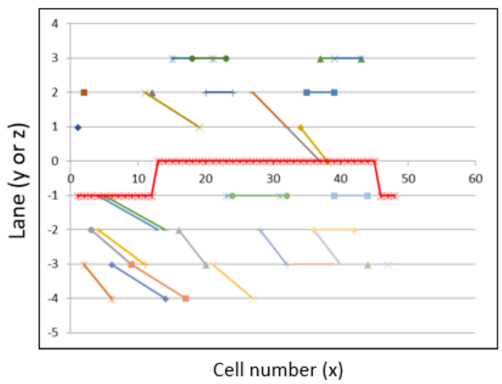

Figure 4a: sample road picture – Major – Police – 0.8 – 0.4

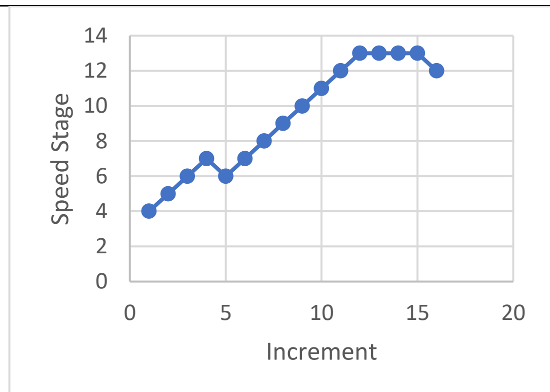

Figure 4b: speed stage vs Increment plot

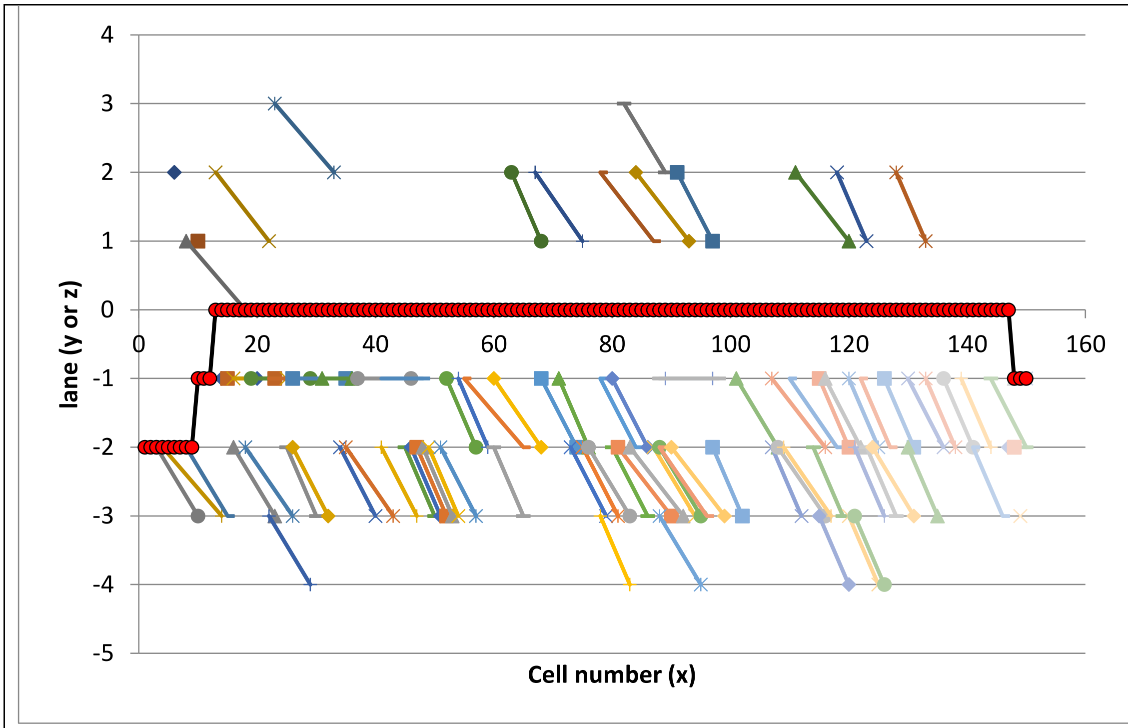

Figure 5: Sample road picture (0.6 mile) - Major – Ambulance – middle - 1.0 – 0.1

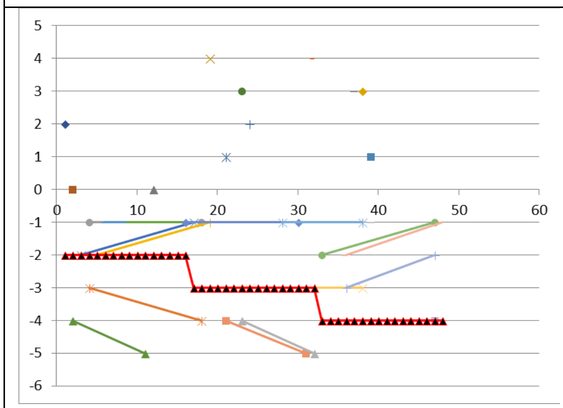

Figure 6a: Sample road picture – Arterial – Police – middle - 0.6 – 0.4

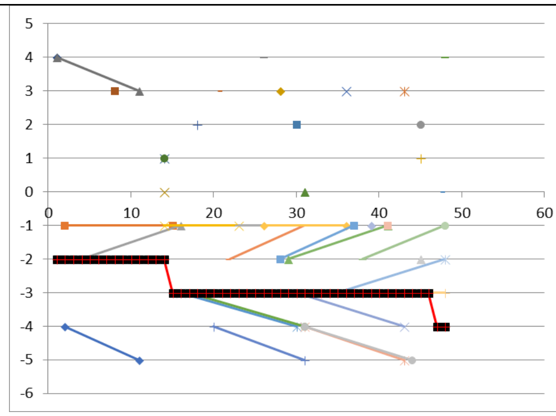

Figure 6b: Sample road picture – Arterial – Police – middle - 0.8 – 0.6

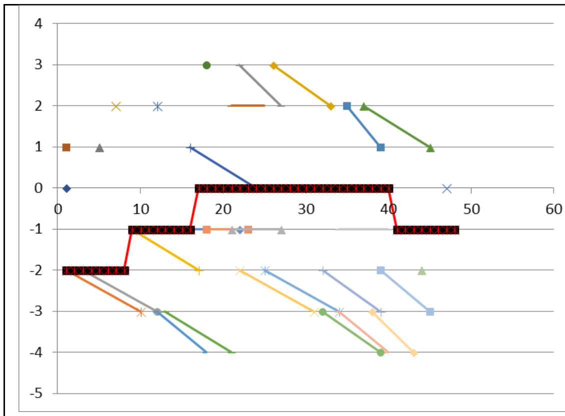

Figure 7a: sample road picture – Major – Police – middle – 0.8 – 0.6

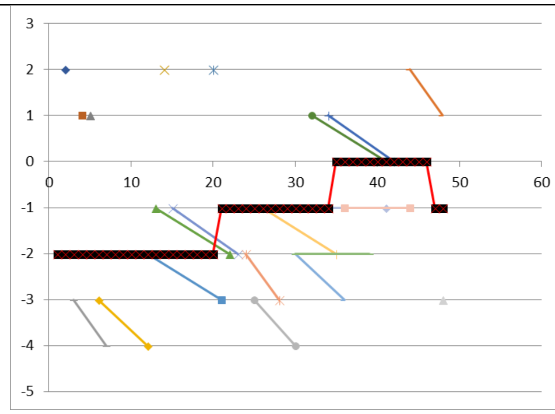

Figure 7b: sample road picture – Major – Police – middle – 0.8 – 0.4

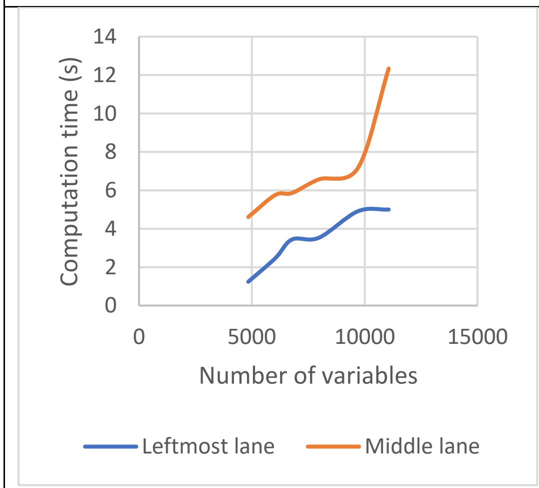

Figure 8a: Computation time vs number of variables – Ambulance

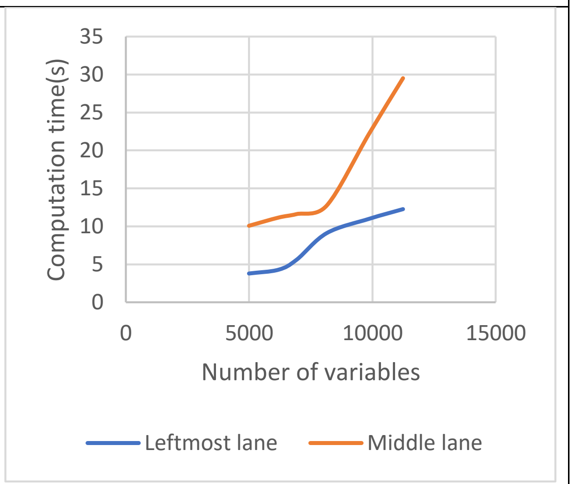

Figure 8b: Computation time vs number of variables - Police

5.2.2 Road composition

Wider roads such as arterials have more route options available. This is because they have more lanes and hence give more lane-change options. So, the contraflow usage is relatively lower in such cases, especially when the traffic density of the normal direction is not very high as observed in figure 9, where the ERV does not enter contraflow even when on the leftmost lane. The contraflow is almost never used when the ERV starts from one of the middle lanes. Contraflow is more frequently used in narrower roads like collectors where police vehicles make use of contraflow even when they start from the rightmost lane, as seen in figures 30a, 32a, 46a and 48a in the appendix. The computation time for arterials is higher due to an increase in the number of variables and constraints, as observed in the graphs 8a-b where the arterial points are the ones with increased number of variables.

The composition of the road does not have any significant effect on the average speeds of the ERV. When the ERV started at the same speed on the leftmost lane on different types of roads, the average speed difference was statistically insignificant as seen in Table 5. To test statistical significance, the chi-square statistic was used as it is an appropriate measure to determine if two sets of values are significantly different from each other [20]. The results on the chi-square statistic between arterial and major collector data yielded a p-value of 0.88, while the p-value on the data between major and minor collectors was 0.93 and the p-value between arterial and minor collectors was also 0.93.

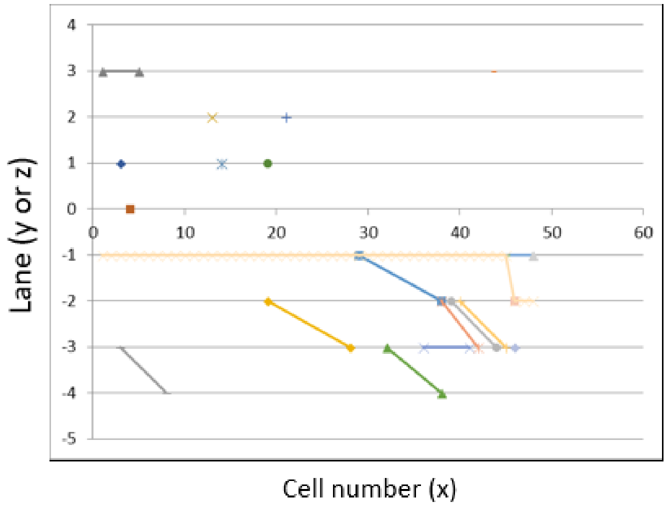

Figure 9: sample road picture – Arterial – Ambulance – left – 0.6 – 0.4

Table 5: Average speeds on different types of roads

v/c normal	v/c contraflow	Arterial avg speed	Major collector avg speed	Minor collector avg speed
0.6	0.4	59.2	58.35	57.58
0.8	0.6	56.86	60.68	58.55
0.8	0.4	59.5	59.73	57.8

5.2.3 Type of ERV

Ambulances make fewer shifts when compared to police vehicles, into the contraflow and fewer lane changes in general due to the greater size of the vehicle. Police vehicles make more maneuvers as compared to ambulances. However, this added ability to maneuver increases the available feasible paths exponentially, resulting in a significant computation time increase. This can be seen in graphs 8b where the computation is significantly higher as compared to 8a, regardless of the starting position of the ERV and the congestion characteristics. Police vehicles are also able to reach higher average speeds as compared to ambulances as seen in figure 10.

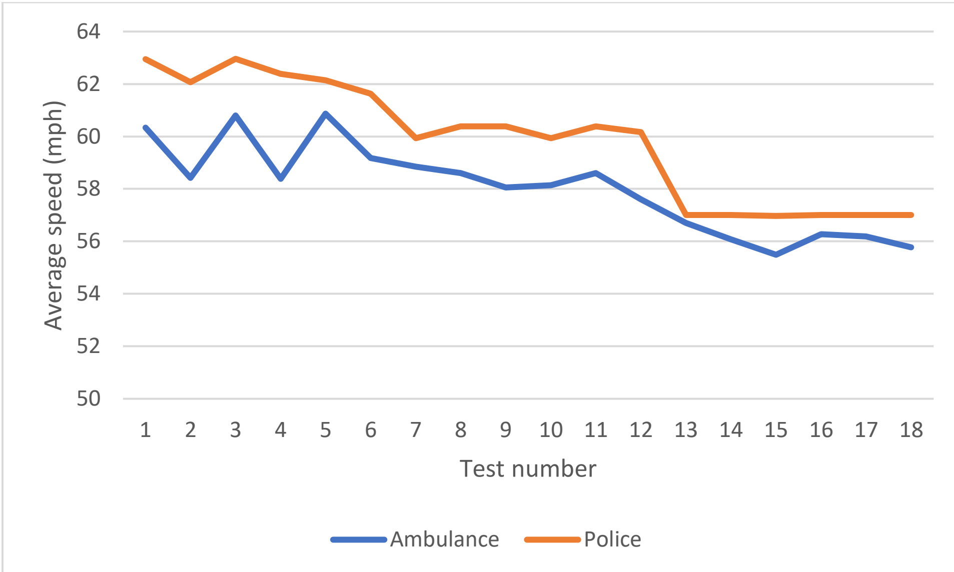

Figure 10: Average speeds - Ambulance vs Police vehicles

5.2.4 Initial speed of the ERV

When the ERV starts at a higher speed, it achieves higher average speeds regardless of the congestion characteristics and its starting position as seen in figure 10 where we see a downward trend in the average speeds for both police and ambulances due to lower starting speeds. The initial speed of the ERV had little effect on the computation time as observed in figure 11, even though it reached the maximum speed quicker when it started faster.

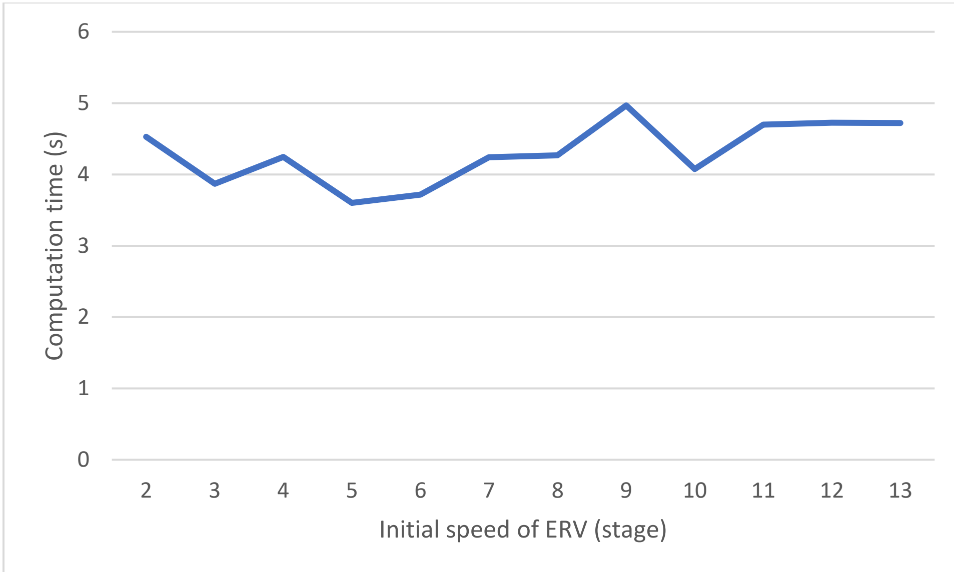

Figure 11: Computation time vs initial ERV speed

5.2.5 Traffic densities

The greater the difference between the traffic densities on the two sides of the road, the greater the usage of contraflow, as seen in figures 6a and 6b where the ERV moved to contraflow even from the middle lane due to higher congestion in the normal direction (v/c = 0.8 in figure 7a and 7b) and sparse traffic in the contraflow (v/c = 0.6 in figure 7a and 0.4 in 7b). Congestion was also major factor which affected computation time, as this was the biggest contributing factor to the number of variables and constraints in the model. With increase in congestion in either direction, there was increase in computation time as seen in figures 8a and 8b where the increase in number of variables let to increase in computation times.

5.2.6 Length of road segment

In graph 12, we observe that the computation time increases exponentially with increase in length of the road segment, with all other parameters fixed. This is logical, as the length of the road segment increases the number of variables and constraints increase as well. If the task of optimizing over an entire link divided into several smaller segments is considered, then, having the length of each segment to be very small means that the formulation is run on many small segments. But, when the length of every road segment is increased, the computation time increases exponentially. From figure 12, it is observed that the optimal length that can be considered for future work is about 40 cells, which provides an increase in length with a negligible increase in computation time.

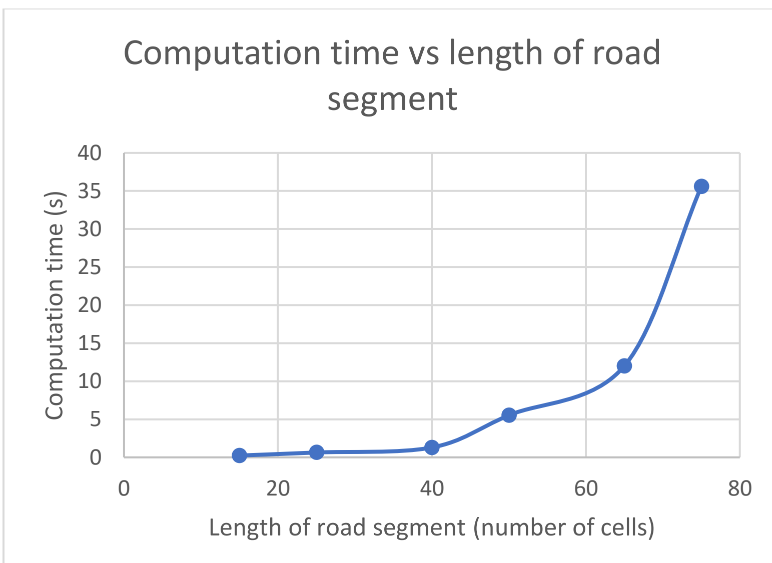

Figure 12: Computation time vs length of road segment

5.2.7 Length of feasible stopping range

The length of the feasible stopping range for each non-ERV was varied and it was found that that parameter did not have any significant effect on either the computation time as seen in figure 13 or the objective function value of the formulation. This maybe due to the fact that while the FSR increases, there is no change in the number of variables.

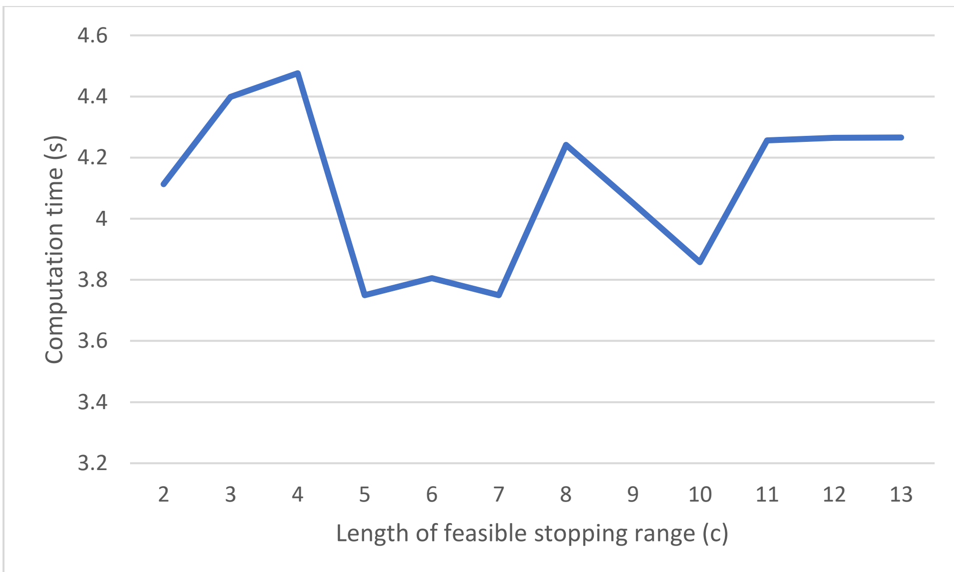

Figure 13: Computation time vs feasible stopping range

5.3 Stage 2: Comparison to non-contraflow strategy

In stage 2, comparison was made on the average ERV speeds, travel times and computation times between the cases when contraflow strategy was used and when it was disabled.

In the tests conducted, the objective function value increased by up to 19 speed units when the congestion in the normal direction was high as observed in figure 14, when the ERV used the contraflow lane. In terms of travel times, there was up to 0.6s for 0.2

miles (6% decrease) improvement when contraflow was used (figure 15b). However, this decrease was only observed when the ERV started in the leftmost lane. The difference in objective function value is greater when the difference in the congestion on both the directions is greater. This trend is observed in figure 15a.

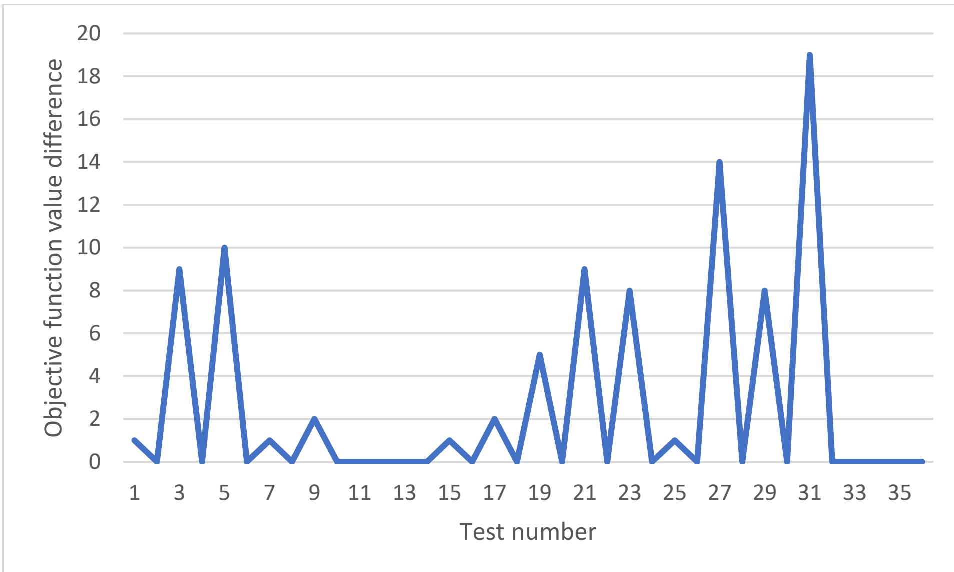

Figure 14: Difference in objective function value between contraflow and non-contraflow strategy

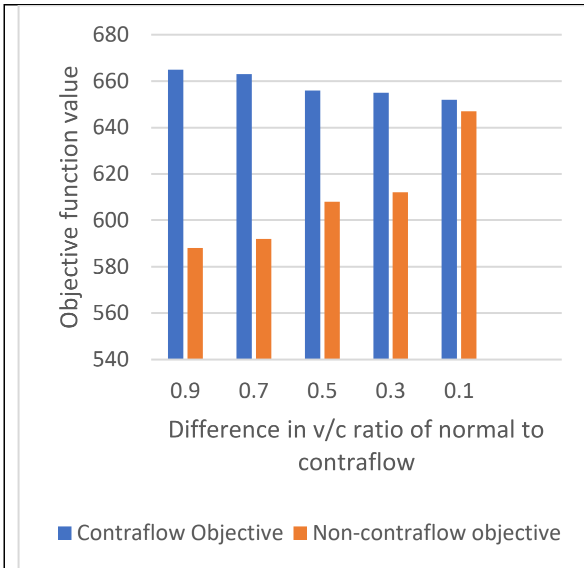

Figure 15a: V/c ratio difference vs objective function value

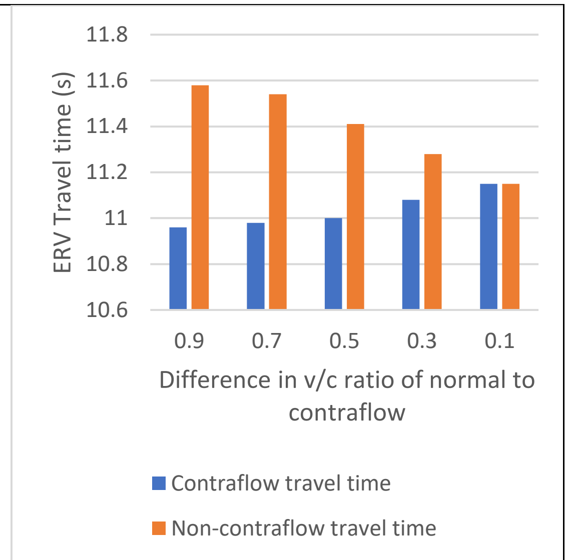

Figure 15b: v/c ratio difference vs travel time

There was almost no difference in travel times observed when the ERV started in the middle or in the rightmost lanes, because the ERV did not use the contraflow lane at all. However, if the congestion difference is very large, the ERV might use the contraflow lane even when it starts from a middle lane as seen in figures 7a and 7b.

When computation times were analyzed, the contraflow strategy takes on average 2.5 times more time to compute the optimal solution than the non-contraflow strategy as seen in figure 16. This can be attributed to the increase in number of constraints, variables, and more possibilities/ routes for the ERV to move in. However, when the contraflow strategy was disabled for all lanes except the leftmost lane, the computation time with contraflow enabled was on average only 1.30 times that of the case when it was disabled, as seen in figure 17.

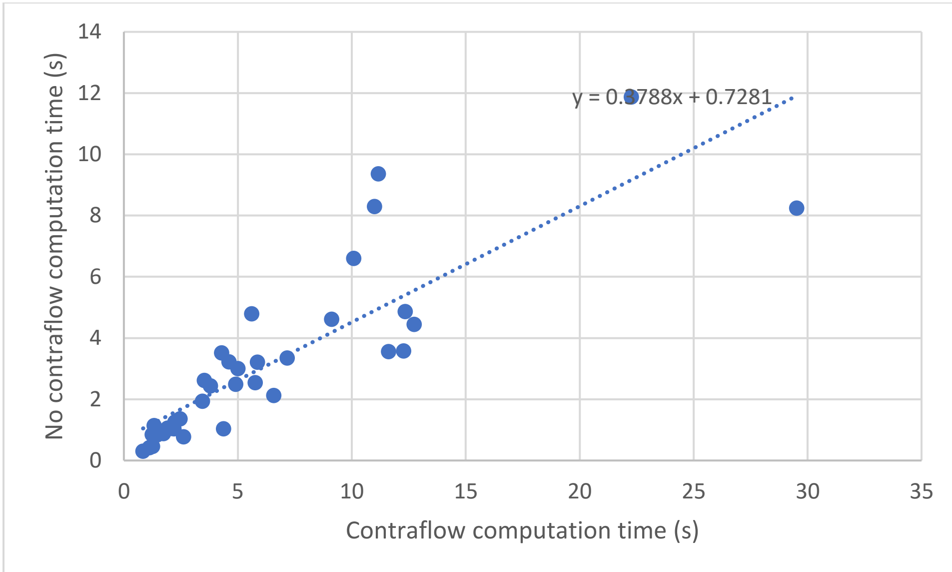

Figure 16: computation time of contraflow vs non-contraflow

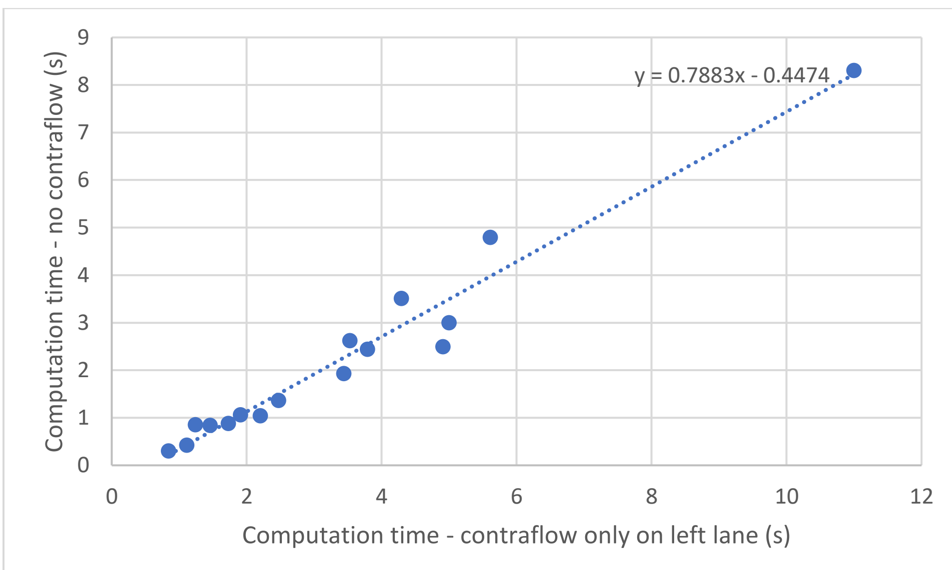

Figure 17: Computation time comparison when contraflow is only enabled on the left lane starts

5.4 Stage 3: Comparison to current practice

In stage 3, comparison was made on the average ERV speeds, travel times and computation times generated using the MILP with contraflow strategy to the current practice of moving vehicles to their nearest lane and not allowing the contraflow option for the ERV.

In the tests conducted, there was up to 16% improvement (2s for 0.2 mile) in travel time and about 10% (5 mph) increase in average speed of ERV. Results of these tests are shown in Table 6. When the congestion difference was higher, the observed improvement of average speeds and travel times was also higher as seen in Table 6.

Table 6: Average speeds and travel times when compared to current practice

v/c normal	v/c contraflow	current practice		Contraflow	
		travel time	avg speed	travel time	avg speed
1	0.1	13.01	54.84	11.02	60.96
0.9	0.2	12.47	55.12	11.6	59.23
0.8	0.3	12.87	53.41	11.56	59.45
0.7	0.4	12.07	56.97	11.6	59.25
0.6	0.5	12.05	57.06	11.48	59.89

The increase in objective function in the tests conducted in stages 2 and 3 also indicate that the space around the ERV when it is traveling across the segment is higher when contraflow is used, since we are also maximizing the environment variables in the objective function.

CHAPTER SIX

OPTIMALITY CUTOFF HEURISTIC

The results from sections 5.3 and 5.4 show that the utilization of contraflow provides the ERV with shorter travel times, but the computation times are higher as well. To reduce the computation time, the solver was instructed to stop the computation when a feasible solution of desired range is obtained. The solver was instructed to stop when the MIP optimality gap was 25%, 20%, 15%, 10% and 5%. This allowed us to obtain solutions that were at least 75%, 80%, 85%, 90% and 95% as good as the optimal solution respectively. Note that while the solution is at least 75% optimal (for example), it might also be optimal or nearly optimal. When the computation times were recorded for these tests, it was found that cutting optimality off at 25% gave results within 3s for all cases tested as shown in figure 18. Next, the quality of the solutions was tested, and it was found that cutting the solutions off at 25% gave nearly optimal solutions in all cases, as seen in figures 19 and 20. The increase in travel time and decrease in average speeds by cutting off the optimality gap was statistically insignificant. The difference between the results obtained on travel times and average speeds by cutting off optimality was negligible, as seen in figures 19 and 20. This meant that the results were acceptable and could be computed in less time (<3s for all cases tested).

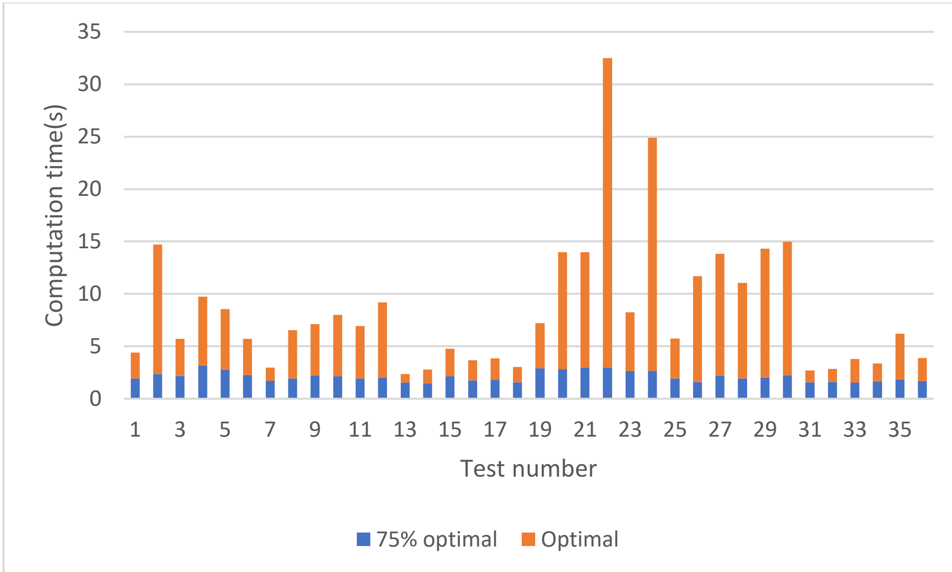

Figure 18: Computation time studies for 75% optimal results with respect to 100% optimal results

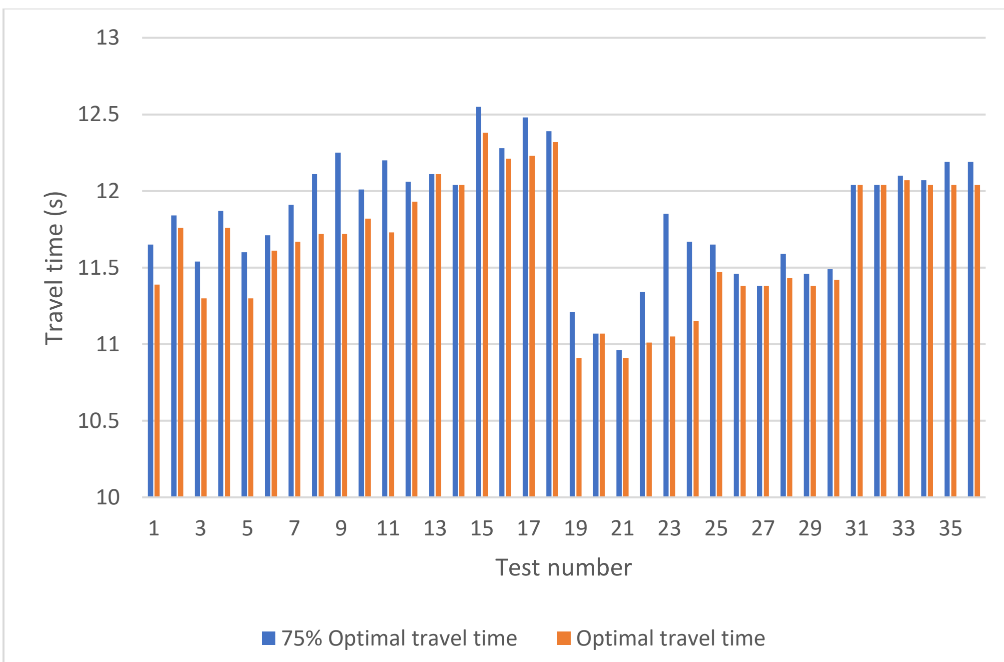

Figure 19: Travel time comparison of heuristic to optimal results

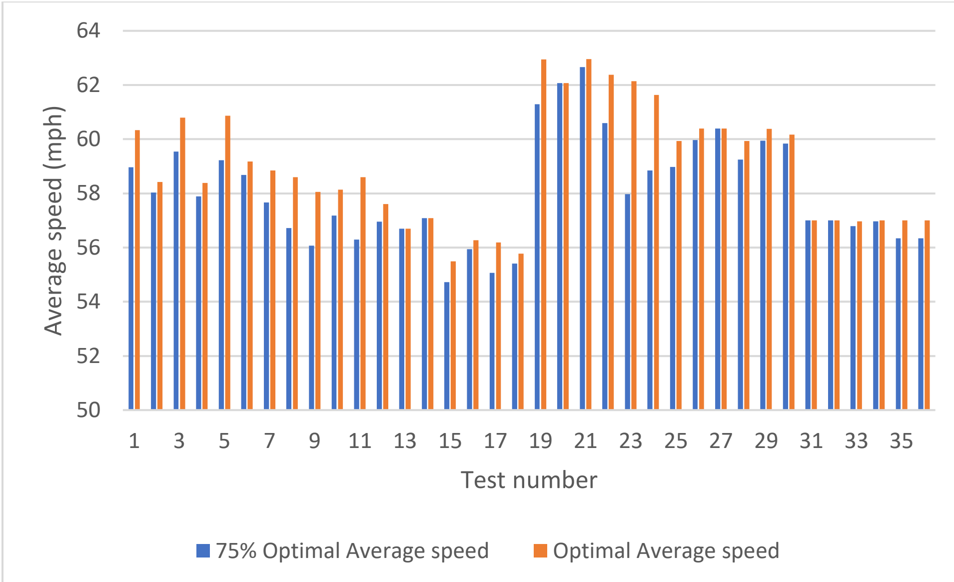

Figure 20: Average speed comparison of heuristic to optimal results

The paths provided by the heuristic and optimal solutions were also compared, and it was found that in most cases (Refer to figures 57-68a and b except 58a-b in the appendix), the path chosen by the heuristic was similar to the path chosen by the optimal solution. In one case (as seen in figures 58a-b in the appendix) when there was a path difference observed, the paths coincided by changing the gap from 25% to 23%. This observation is attributed to chance. Barring this one case, the only change that was observed between the two solutions was the point at which the lane change happened. Also, whenever the heuristic suggested the use of contraflow, the optimal solution also suggested the same. This gives credibility to the heuristic in the sense that the paths that it provides are also similar to the optimal paths.

CHAPTER SEVEN

CONCLUSIONS AND FUTURE WORK

In this paper, initial work from [5] has been revised and extended to include the possibility for the ERV to utilize the contraflow segment of the road as well. Improvements have been made on the existing model by increasing the computational efficiency as well as changing the passing/weaving constraints to provide additional safety. Most importantly however, an extension has been developed to utilize the contraflow segment of the road and rules developed.

The inputs to the model are the current positions and speeds of the ERV and non-ERVs on both sides of the road and their braking capabilities. These inputs are pre-processed as explained to provide minimum stopping distances for each non-ERV and fed into the MILP for finding the optimal path for the ERV to take as well as the positions on the road for every non-ERV to move to, in the segment.

From the experiments conducted, the use of the contraflow strategy provides significant improvement (up to 16% or 2s for 0.2 miles) over the current practice as well as the normal-direction-only-strategy (up to 12% or 1.5s for 0.2 miles) developed in [6]. This can also be concluded from the frequent use of contraflow in the experiments conducted. Contraflow usage was optimal even when the ERV had to make 2 or 3 lanes shifts to enter the contraflow. It must also be noted that safety has not been compromised and there is no chance of head on collisions with 100% market penetration for the technology and compliance with the instructions, since no non-ERV in the contraflow can use the leftmost lane in the contraflow when the ERV enters it.

The practical usability of the formulation has been considered by studying the computation time and developing an optimality cutoff heuristic which gives near-optimal results in usable computation times.

Future work includes developing strategies to run this formulation on multiple sequences of links and obtaining the fastest paths for the ERV from its source to its destination.

APPENDIX

Results from experiments conducted in Stage 1:

Arterial – Ambulance – 0.6 – 0.4

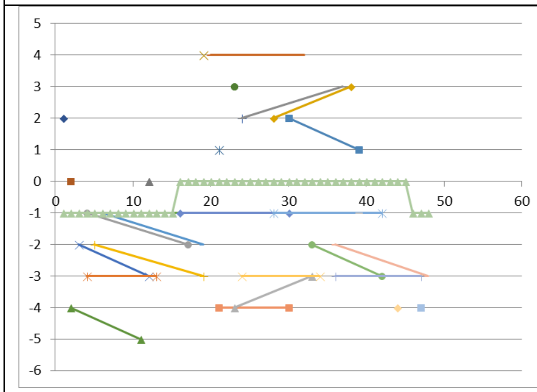

Figure 21a: Arterial – Ambulance – left – 0.6 – 0.4

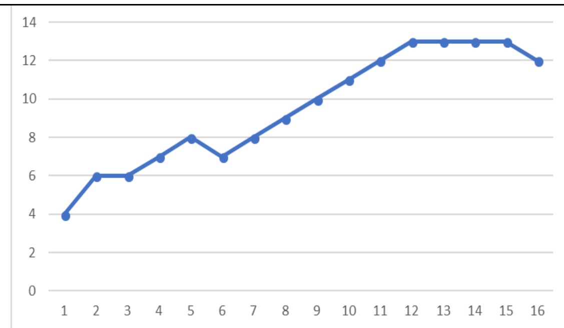

Figure 21b: Speed stage vs increment for case 21a

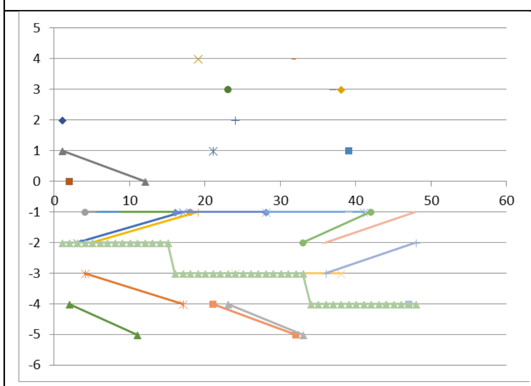

Figure 22a: Arterial - Ambulance - middle - 0.6 - 0.4

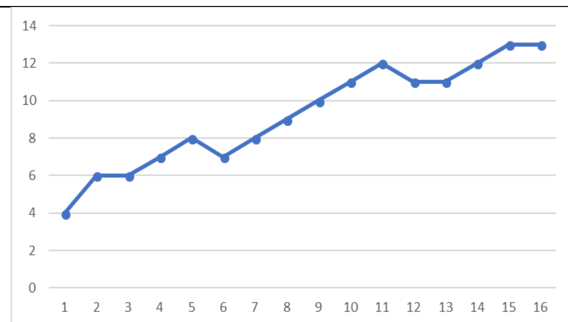

Figure 22b: Speed stage vs increment for case 22a

Arterial – Ambulance – 0.8 – 0.4

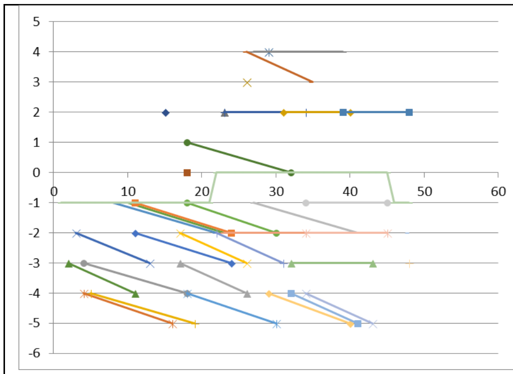

Figure 23a: Arterial - Ambulance - left - 0.8 - 0.4

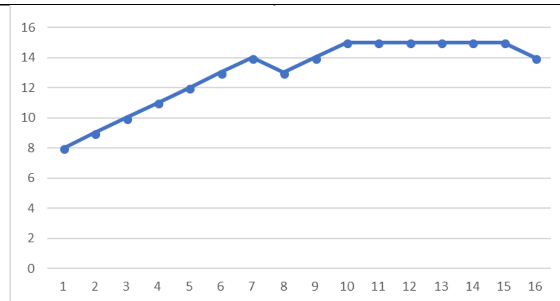

Figure 23b: Speed stage vs increment for case 23a

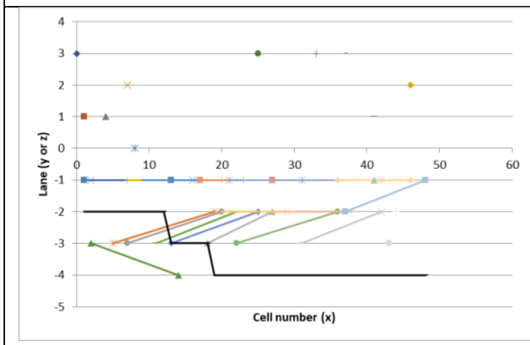

Figure 24a: Arterial - Ambulance - middle - 0.8 - 0.4

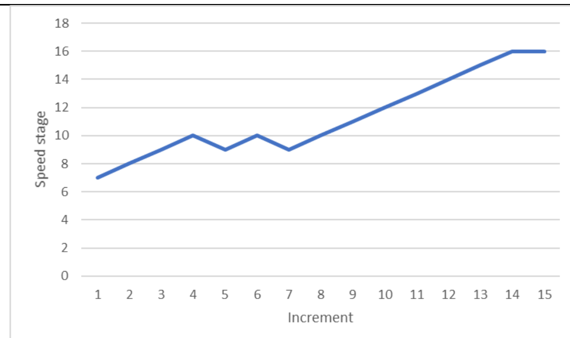

Figure 24b: Speed stage vs increment for case 24a

Arterial – Ambulance – 0.8 – 0.6

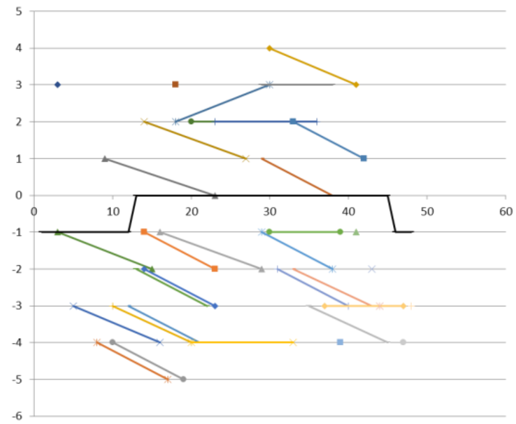

Figure 25a: Arterial - Ambulance - left - 0.8 - 0.6

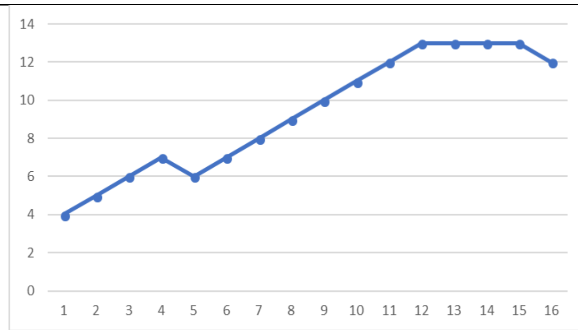

Figure 25b: Speed stage vs increment for case 25a

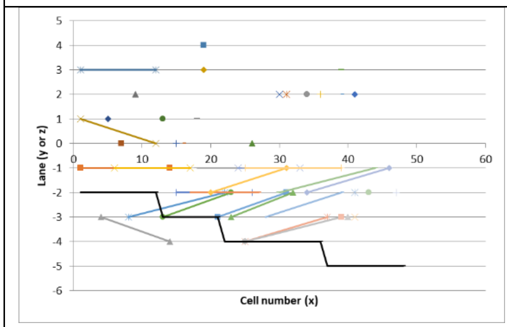

Figure 26a: Arterial - Ambulance - middle - 0.8 - 0.6

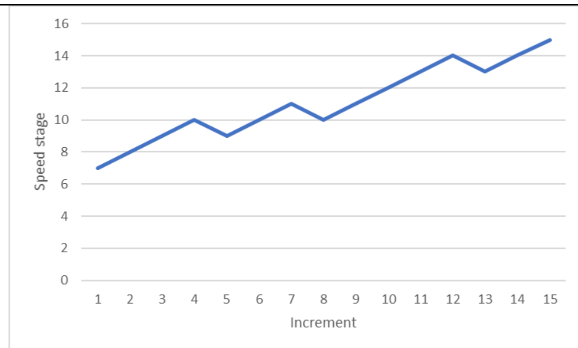

Figure 26b: Speed stage vs increment for case 26a

Major Collector – Ambulance – 0.6 – 0.4

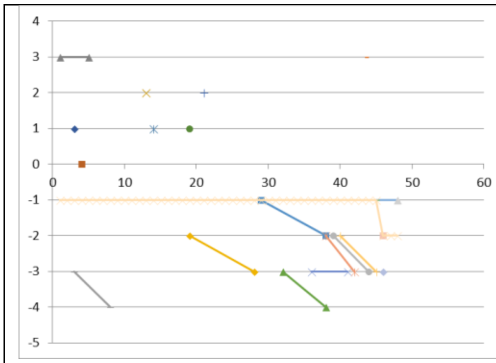 Figure 27a: Major - Ambulance - left - 0.6 - 0.4	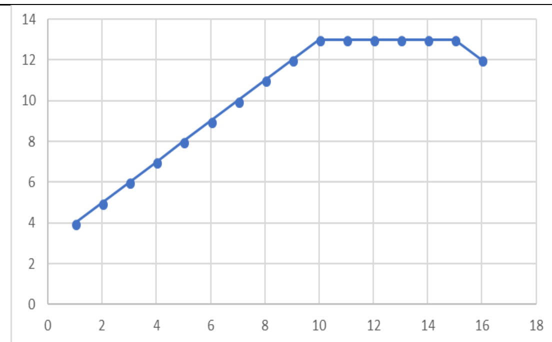 Figure 27b: Speed stage vs increment for case 27a
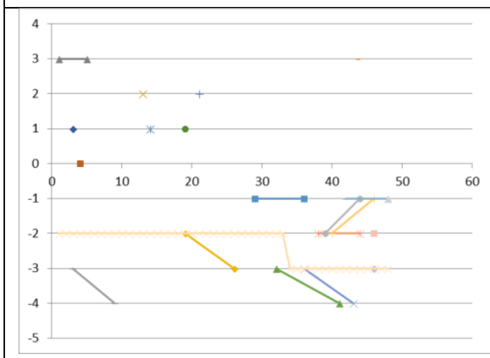 Figure 28a: Major - Ambulance - middle - 0.6 - 0.4	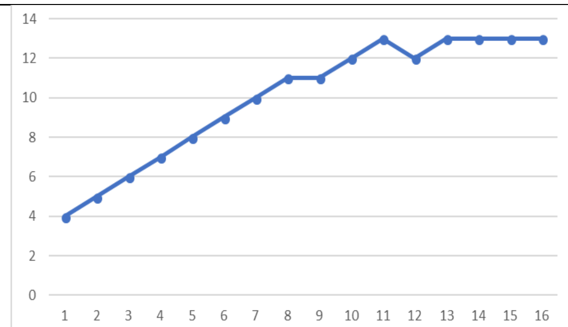 Figure 28b: Speed stage vs increment for case 28a
Major Collector – Ambulance – 0.8 – 0.4	

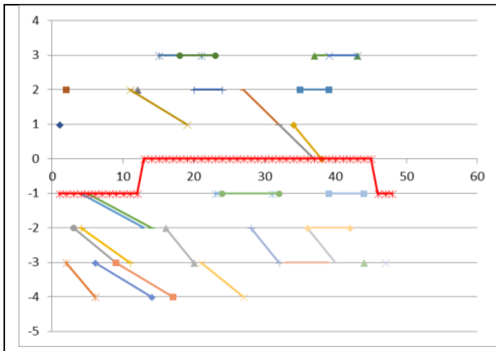

Figure 29a: Major - Ambulance - left - 0.8 - 0.4

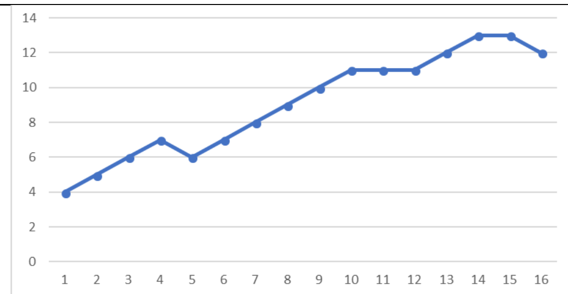

Figure 29b: Speed stage vs increment for case 29a

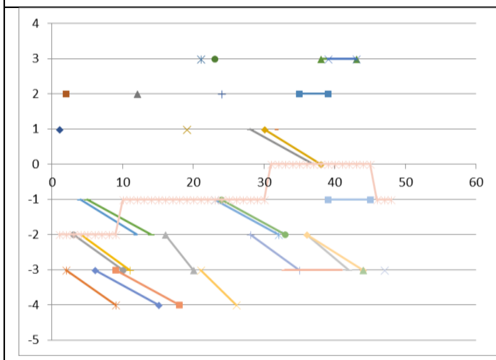

Figure 30a: Major - Ambulance - middle - 0.8 - 0.4

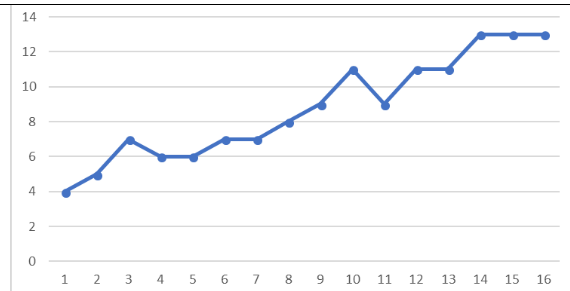

Figure 30b: Speed stage vs increment for case 30a

Major Collector – Ambulance – 0.8 – 0.6

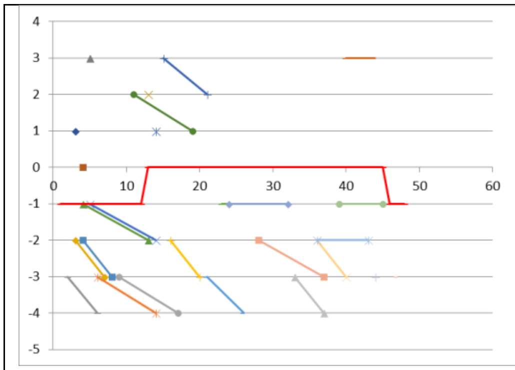

Figure 31a: Major - Ambulance - left - 0.8 - 0.6

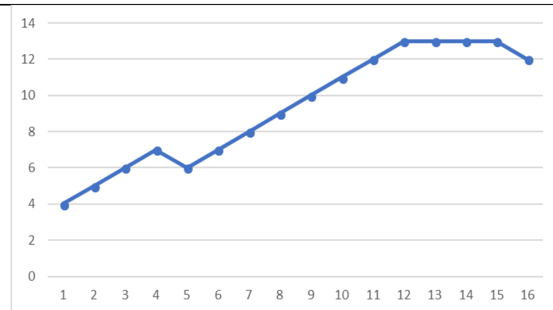

Figure 31b: Speed stage vs increment for case 31a

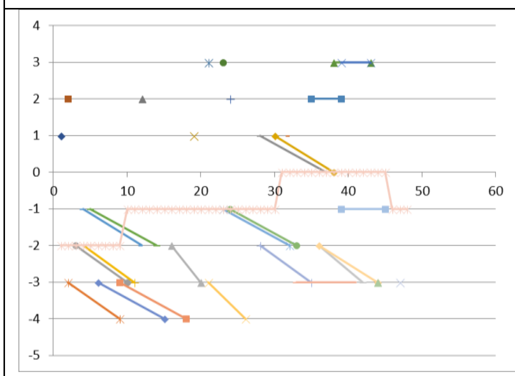

Figure 32a: Major - Ambulance - middle - 0.8 - 0.6

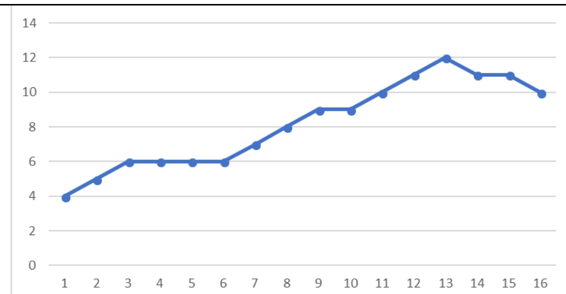

Figure 32b: Speed stage vs increment for case 32a

Minor Collector – Ambulance – 0.6 – 0.4

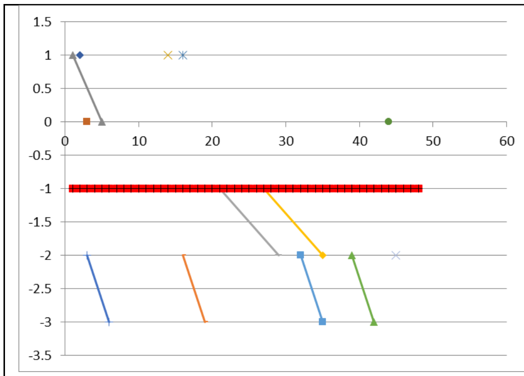 Figure 33a: Minor - Ambulance - left - 0.6 - 0.4	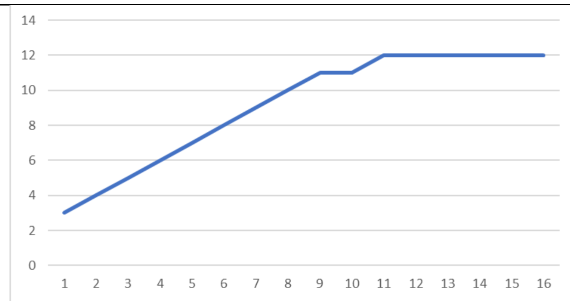 Figure 33b: Speed stage vs increment for case 33a
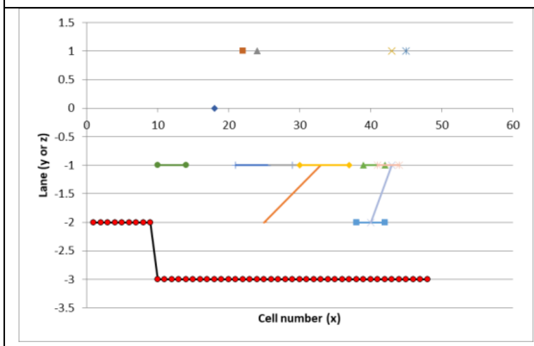 Figure 34a: Minor - Ambulance - middle - 0.6 - 0.4	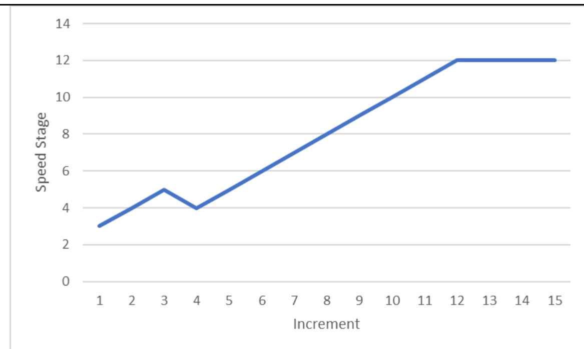 Figure 34b: Speed stage vs increment for case 34a
Minor Collector – Ambulance – 0.8 – 0.4	

<table>
<tr>
<td>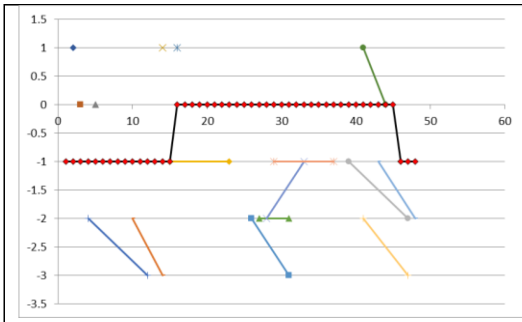

Figure 35a: Minor - Ambulance - left - 0.8 - 0.4</td>
<td>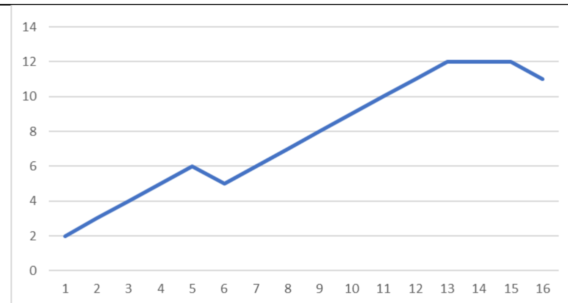

Figure 35b: Speed stage vs increment for case 35a</td>
</tr>
<tr>
<td>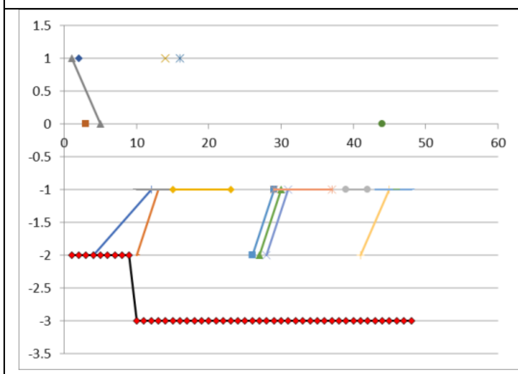

Figure 36a: Minor - Ambulance - middle - 0.8 - 0.4</td>
<td>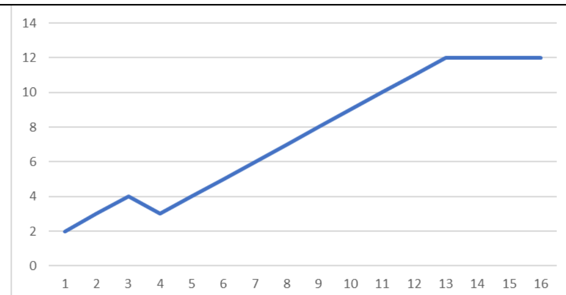

Figure36b: Speed stage vs increment for case 36a</td>
</tr>
<tr>
<td colspan="2">Minor Collector – Ambulance – 0.8 – 0.6</td>
</tr>
</table>

<table>
<tr>
<td>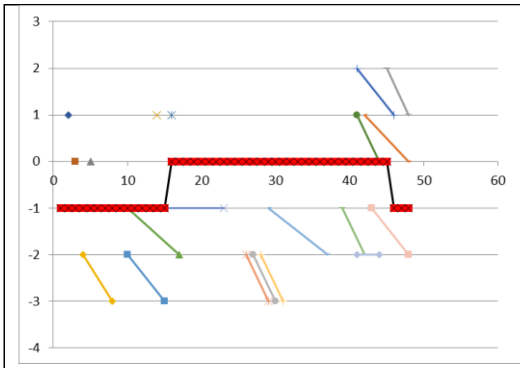

Figure 37a: Minor - Ambulance - left - 0.8 - 0.6</td>
<td>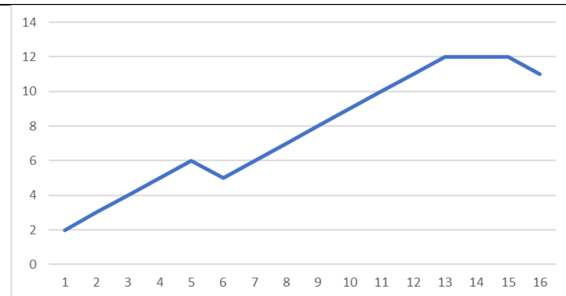

Figure 37b: Speed stage vs increment for case 37a</td>
</tr>
<tr>
<td>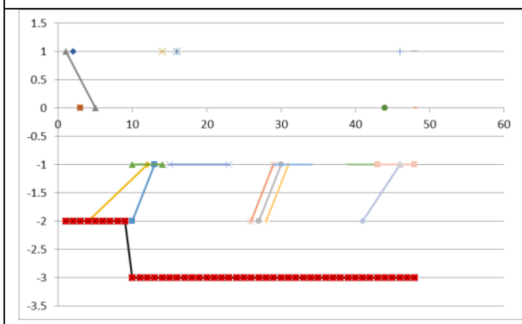

Figure 38a: Minor - Ambulance - middle - 0.8 - 0.6</td>
<td>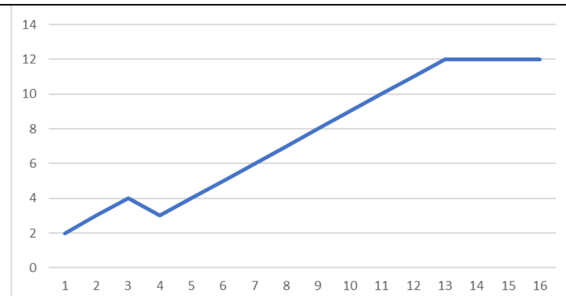

Figure 38b: Speed stage vs increment for case 38a</td>
</tr>
<tr>
<td colspan="2">Arterial – Police – 0.6 – 0.4</td>
</tr>
</table>

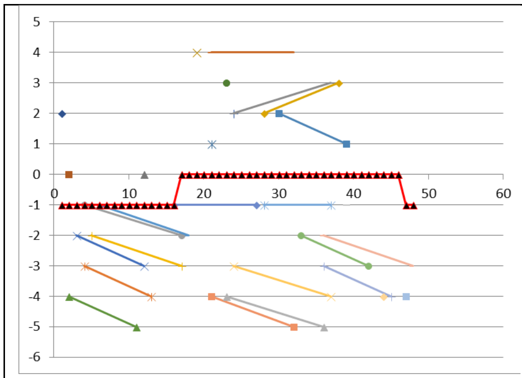

Figure 39a: Arterial - Police - left - 0.6 - 0.4

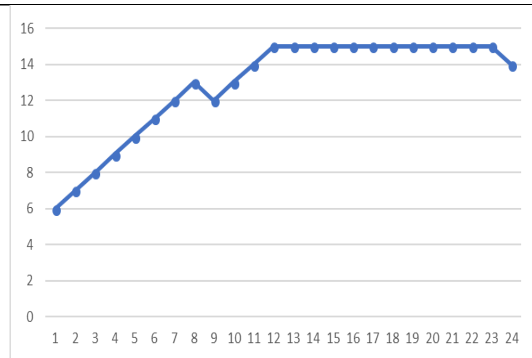

Figure 39b: Speed stage vs increment for case 39a

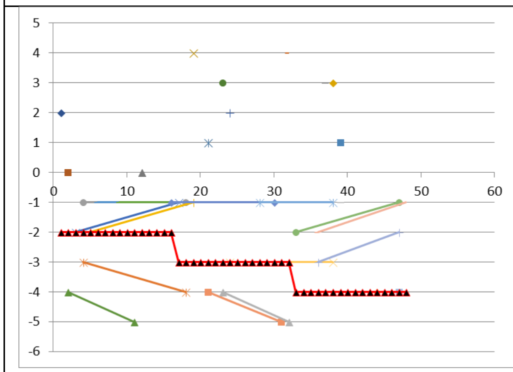

Figure 40a: Arterial - Police - middle - 0.6 - 0.4

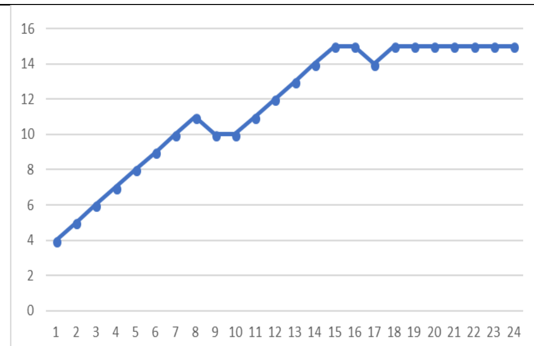

Figure 40b: Speed stage vs increment for case 40a

Arterial – Police – 0.8 – 0.4

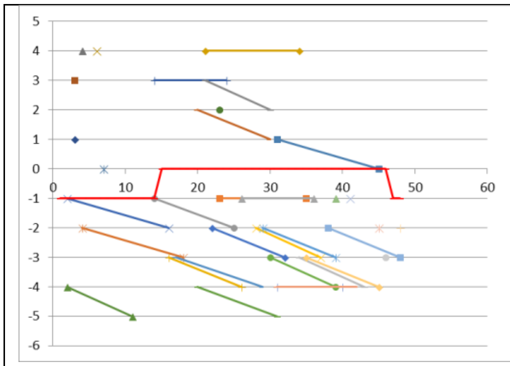

Figure 41a: Arterial - Police - left - 0.8 - 0.4

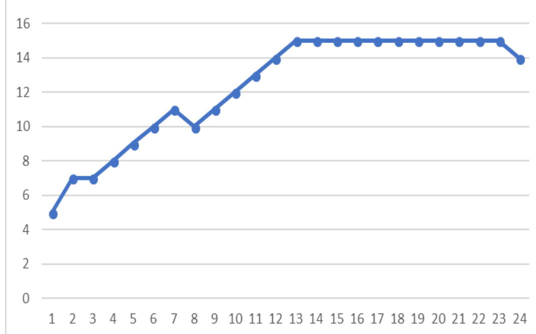

Figure 41b: Speed stage vs increment for case 41a

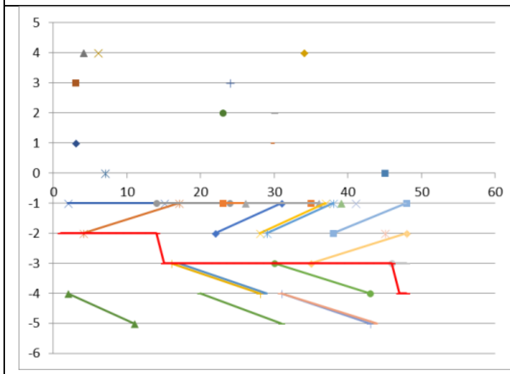

Figure 42a: Arterial - Police - middle - 0.8 - 0.4

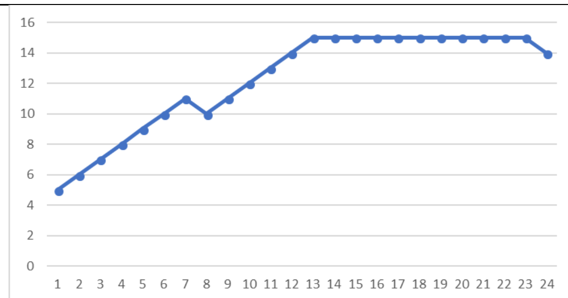

Figure 42b: Speed stage vs increment for case 42a

Arterial – Police – 0.8 – 0.6

<table>
<tr>
<td>
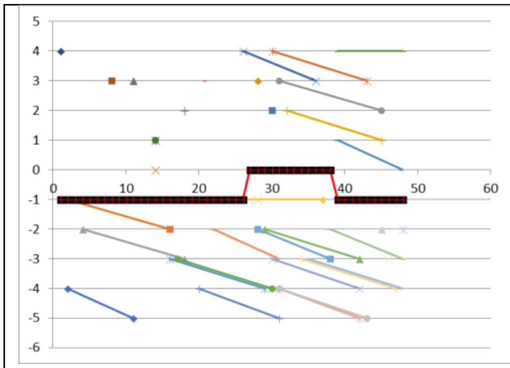

Figure 43a: Arterial - Police - left - 0.8 - 0.6
</td>
<td>
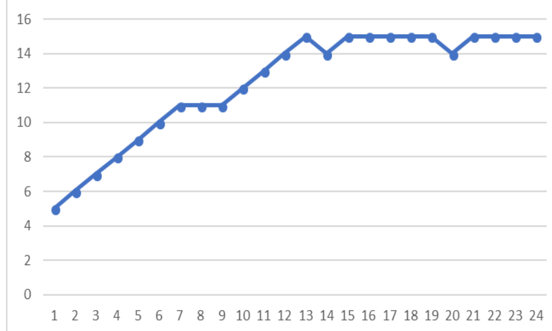

Figure 43b: Speed stage vs increment for case 43a
</td>
</tr>
<tr>
<td>
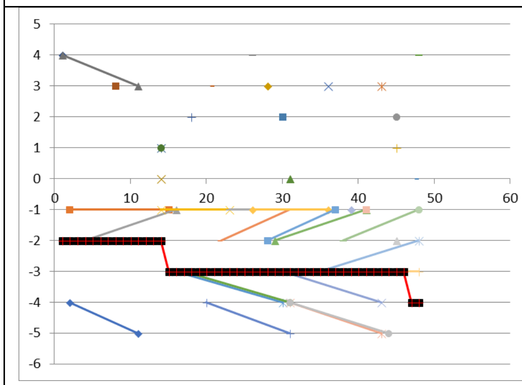

Figure 44a: Arterial - Police - middle - 0.8 - 0.6
</td>
<td>
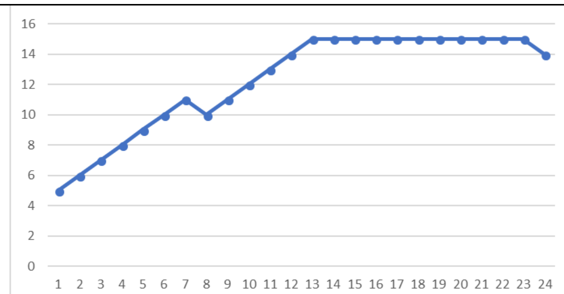

Figure 44b: Speed stage vs increment for case 44a
</td>
</tr>
<tr>
<td colspan="2">Major Collector – Police – 0.6 – 0.4</td>
</tr>
</table>

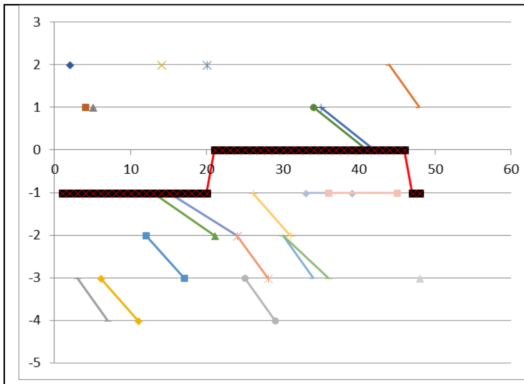

Figure 45a: Major - Police - left - 0.6 - 0.4

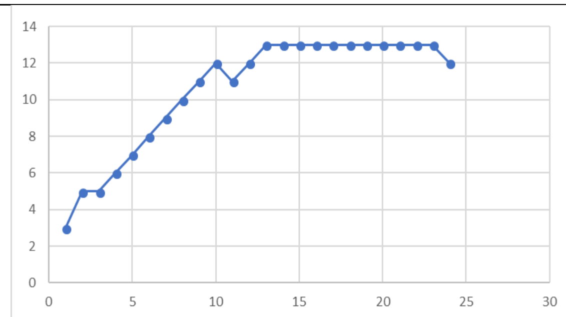

Figure 45b: Speed stage vs increment for case 45a

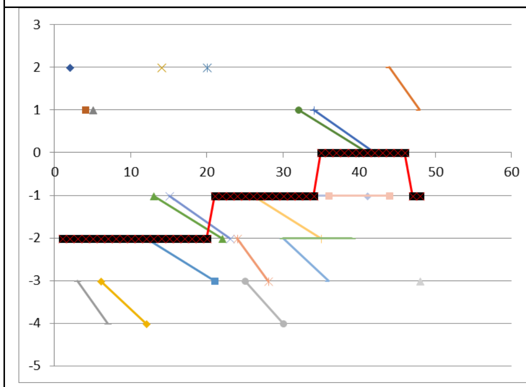

Figure 46a: Major - Police - middle - 0.6 - 0.4

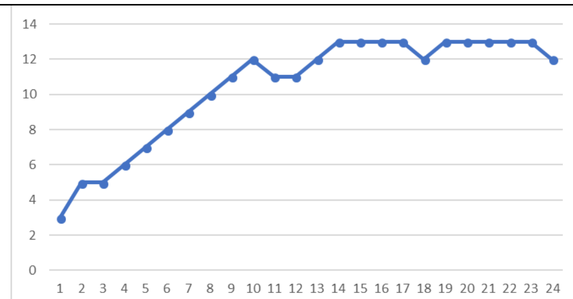

Figure 46b: Speed stage vs increment for case 46a

Major Collector – Police – 0.8 – 0.4

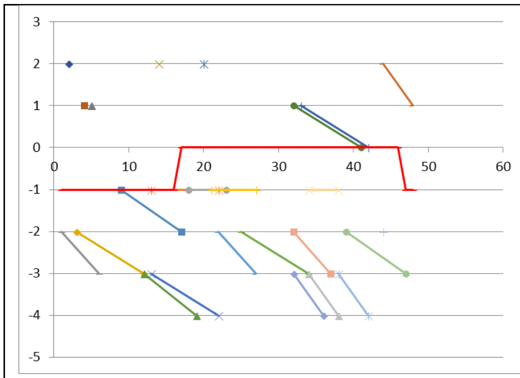

Figure 47a: Major - Police - left - 0.8 - 0.4

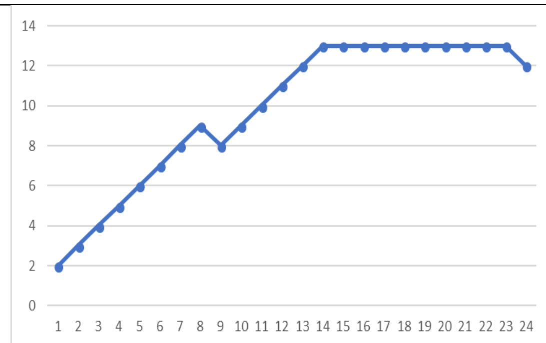

Figure 47b: Speed stage vs increment for case 47a

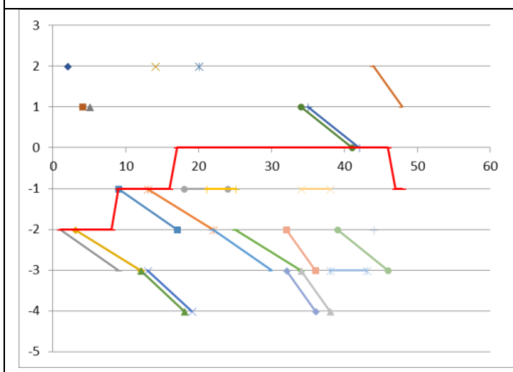

Figure 48a: Major - Police - middle - 0.8 - 0.4

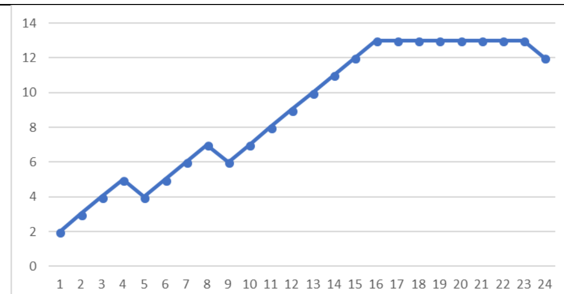

Figure 48b: Speed stage vs increment for case 48a

Major Collector – Police – 0.8 – 0.6

<table>
<tr>
<td>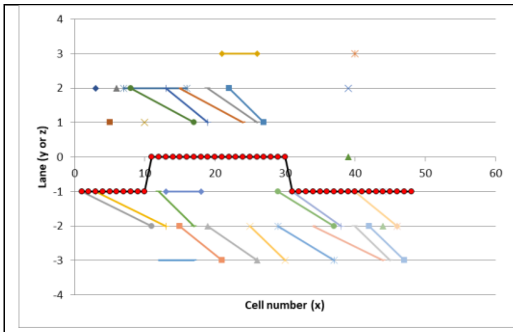

Figure 49a: Major - Police - left - 0.8 - 0.6</td>
<td>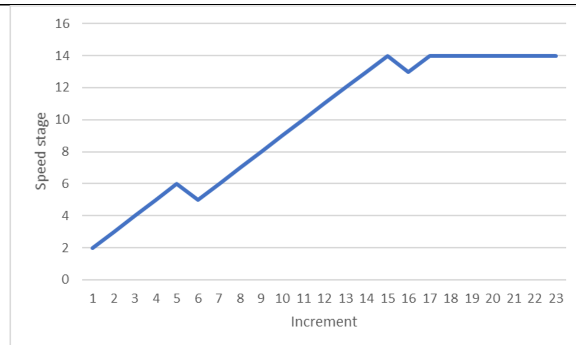

Figure 49b: Speed stage vs increment for case 49a</td>
</tr>
<tr>
<td>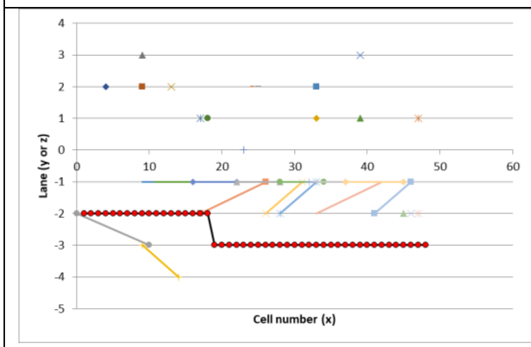

Figure 50a: Major - Police - middle - 0.8 - 0.6</td>
<td>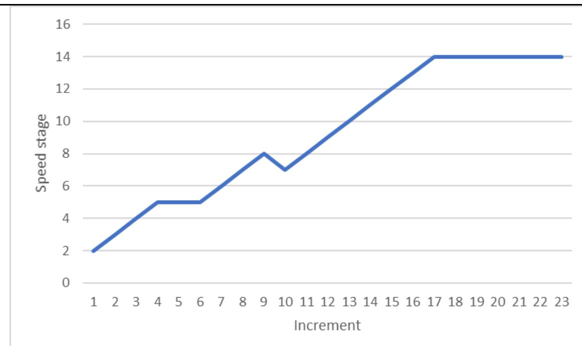

Figure 50b: Speed stage vs increment for case 50a</td>
</tr>
<tr>
<td colspan="2">Minor Collector – Police – 0.6 – 0.4</td>
</tr>
</table>

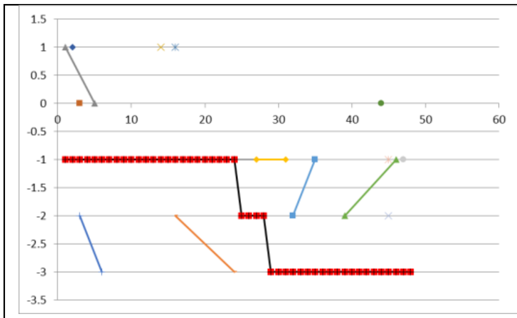

Figure 51a: Minor - Police - left - 0.6 - 0.4

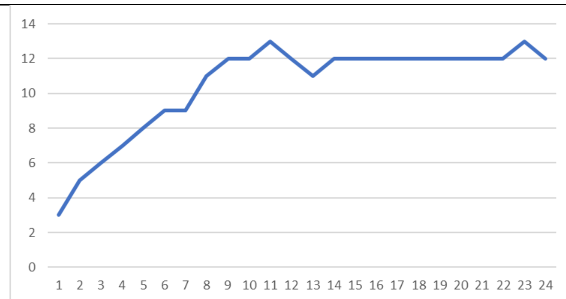

Figure 51b: Speed stage vs increment for case 51a

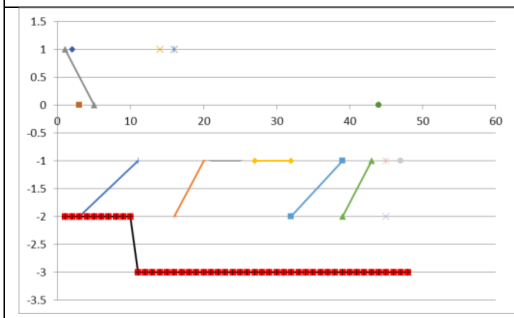

Figure 52a: Minor - Police - middle - 0.6 - 0.4

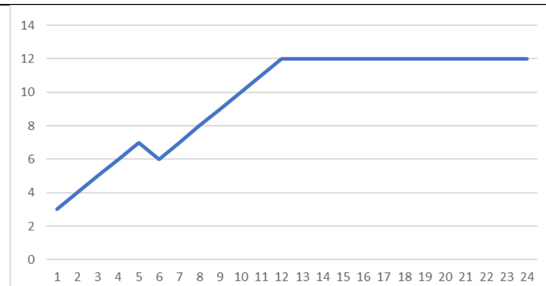

Figure 52b: Speed stage vs increment for case 52a

Minor Collector – Police – 0.8 – 0.4

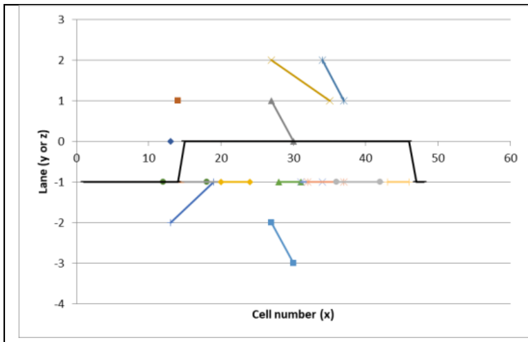

Figure 53a: Minor - Police - left - 0.8 - 0.4

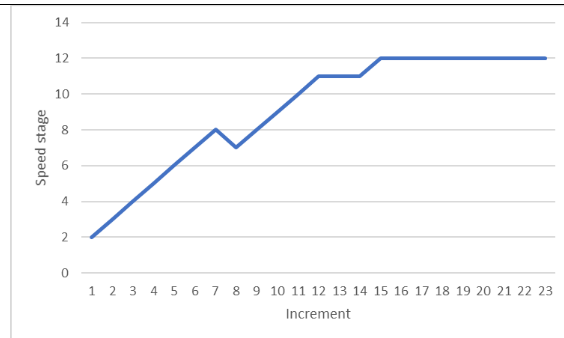

Figure 53b: Speed stage vs increment for case 53a

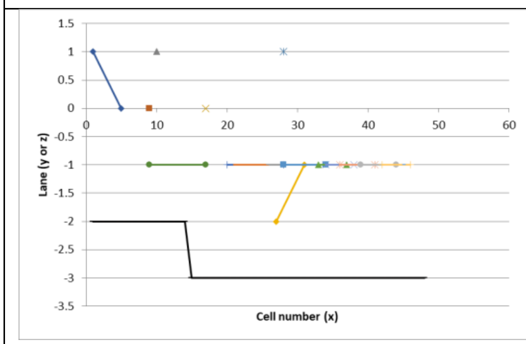

Figure 54a: Minor - Police - middle - 0.8 - 0.4

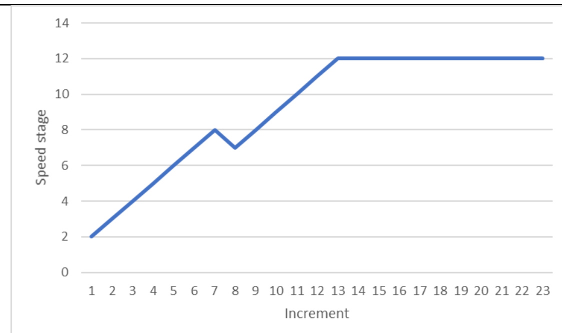

Figure 54b: Speed stage vs increment for case 54a

Minor Collector – Police – 0.8 – 0.6

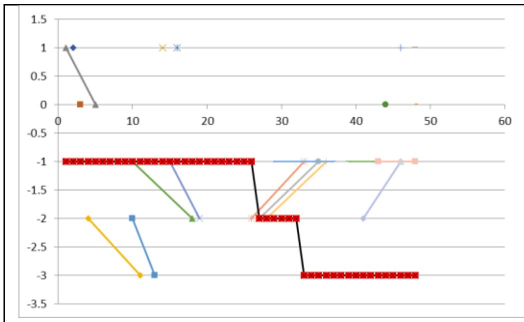

Figure 55a: Minor - Police - left - 0.8 - 0.6

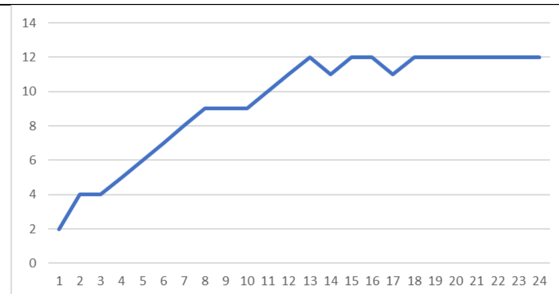

Figure 55b: Speed stage vs increment for case 55a

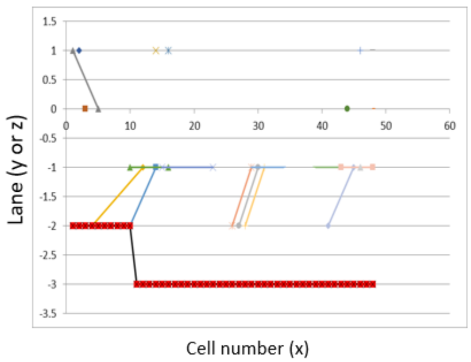

Figure 56a: Minor - Police - middle - 0.8 - 0.6

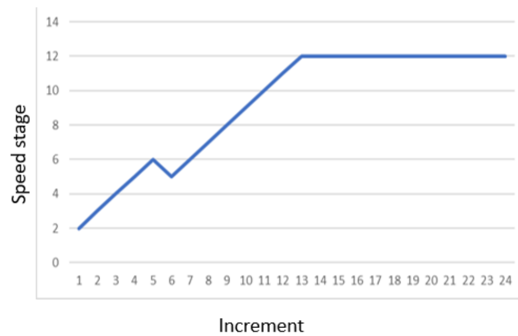

Figure 56a: Speed stage vs increment for case 56a

Results from tests conducted to determine differences in paths between the heuristic and optimal solutions:

Heuristic path	Optimal path
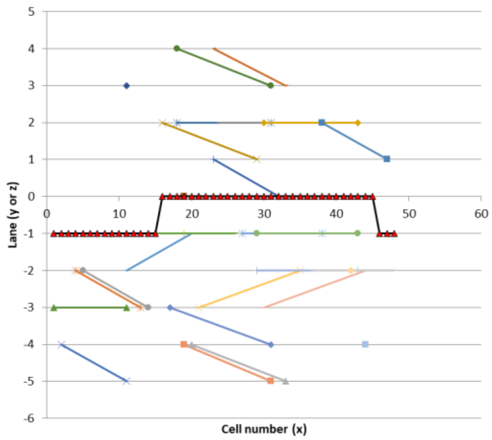 Figure 57a: Arterial - Ambulance - left - 0.6 - 0.4 – Heuristic	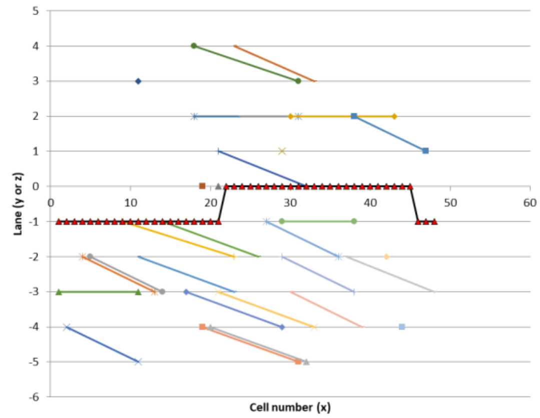 Figure 57b: Arterial - Ambulance - left - 0.6 - 0.4 - Optimal
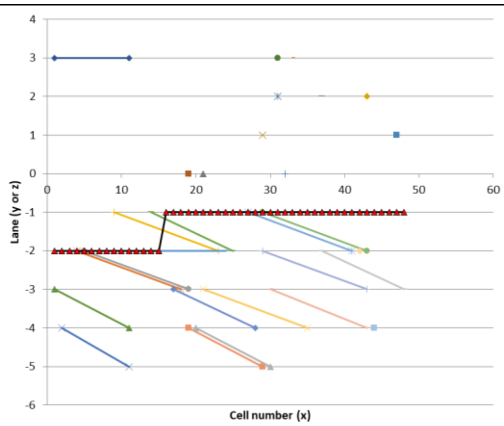 Figure 58a: Arterial - Ambulance - middle - 0.6 - 0.4 – Heuristic	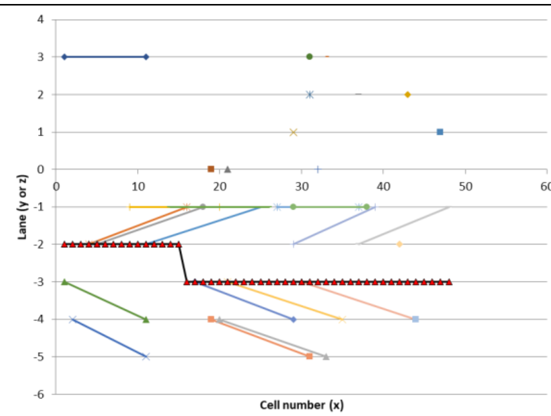 Figure 58b: Arterial - Ambulance - middle - 0.6 - 0.4 - Optimal

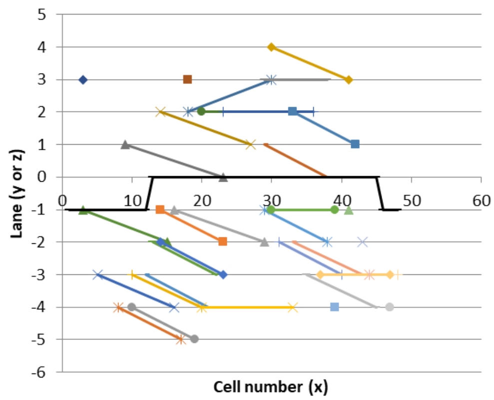

Figure 59a: Arterial - Ambulance - left - 0.8 - 0.4 – heuristic

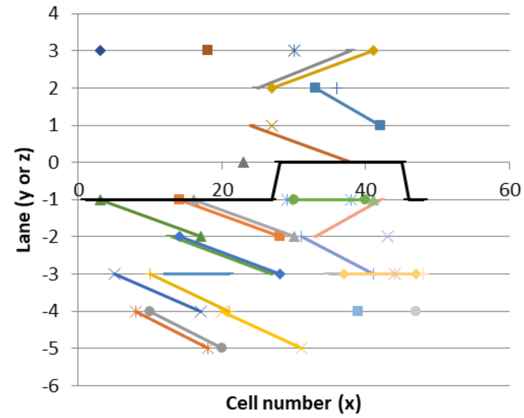

Figure 59b: Arterial - Ambulance - left - 0.8 - 0.4 - Optimal

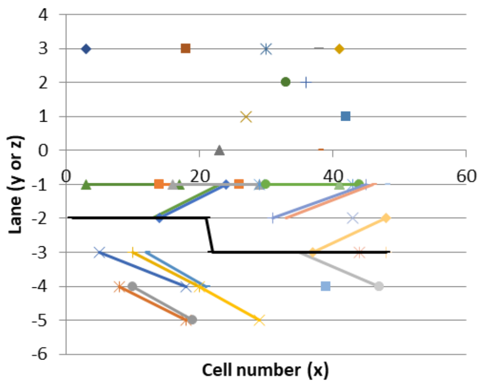

Figure 60a: Arterial - Ambulance - middle - 0.8 - 0.4 – Heuristic

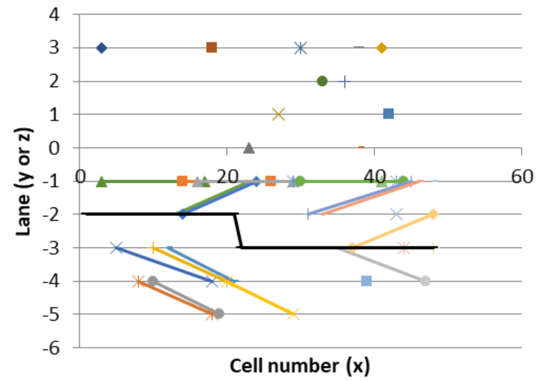

Figure 60b: Arterial - Ambulance - middle - 0.8 - 0.4 - Optimal

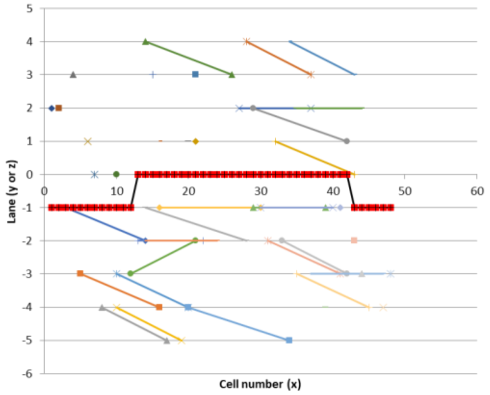

Figure 61a: Arterial - Ambulance - left - 0.8 - 0.6 – Heuristic

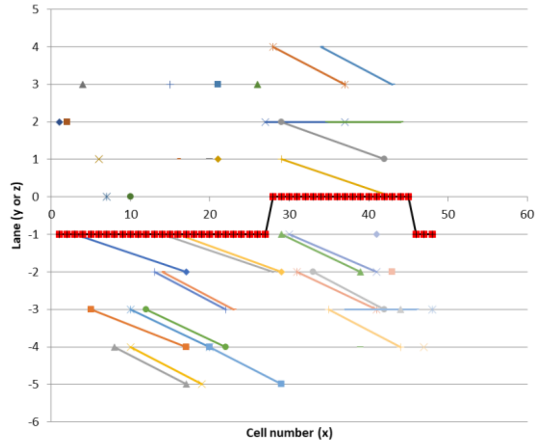

Figure 61b: Arterial - Ambulance - left - 0.8 - 0.6 - Optimal

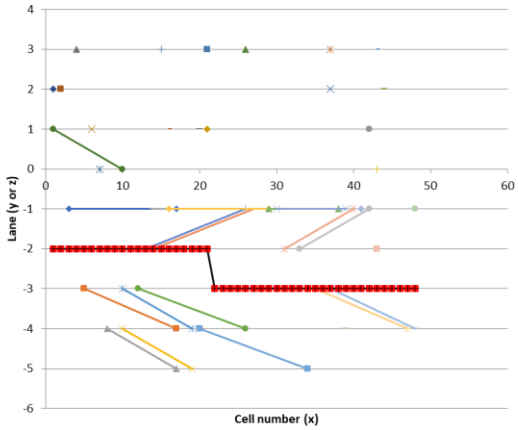

Figure 62a: Arterial - Ambulance - middle - 0.8 - 0.6 – Heuristic

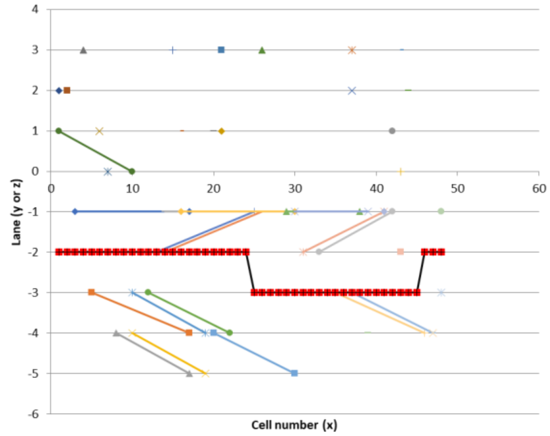

Figure 62b: Arterial - Ambulance - middle - 0.8 - 0.6 - Optimal

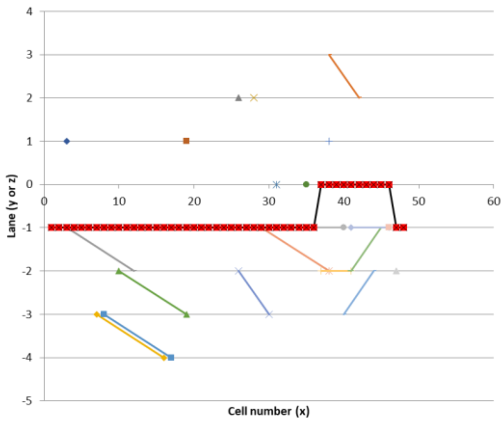

Figure 63a: Major - Police - left - 0.6 - 0.4 - Heuristic

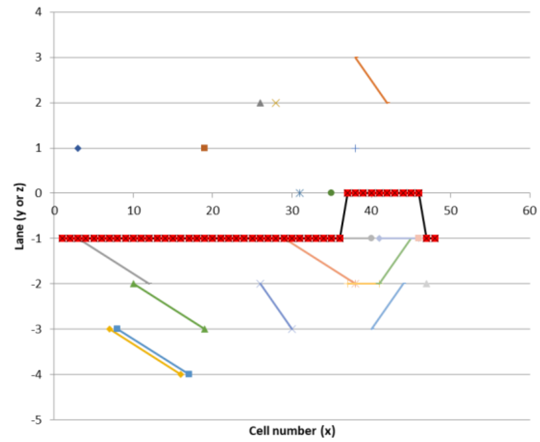

Figure 63b: Major - Police - left - 0.6 - 0.4 – Optimal

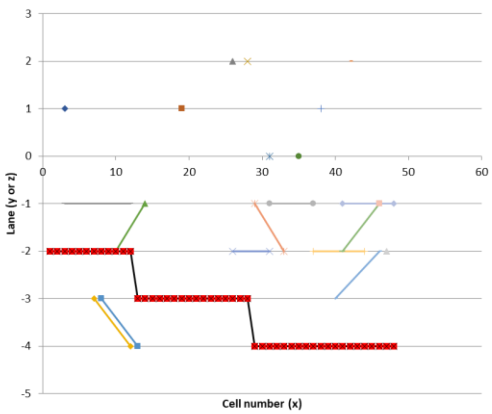

Figure 64a: Major - Police - middle - 0.6 - 0.4 – Heuristic

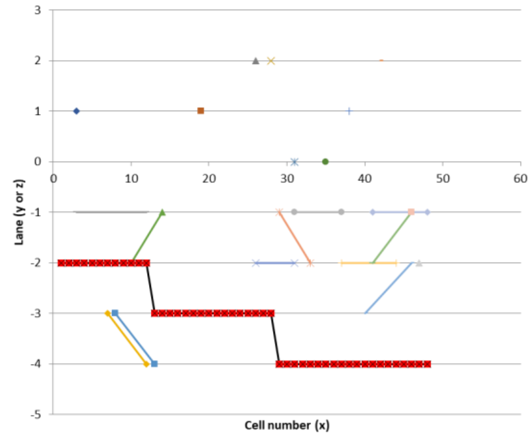

Figure 64b: Major - Police - middle - 0.6 - 0.4 - Optimal

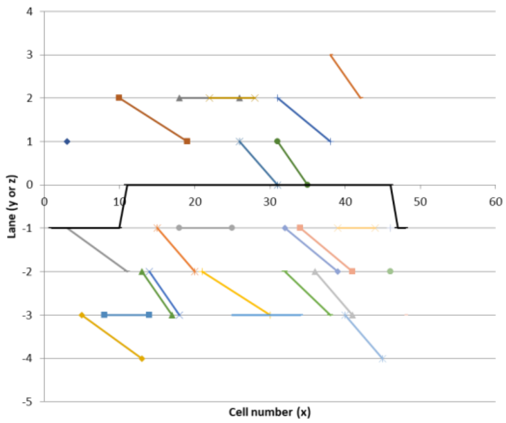

Figure 65a: Major - Police - left - 0.8 - 0.4 - Heuristic

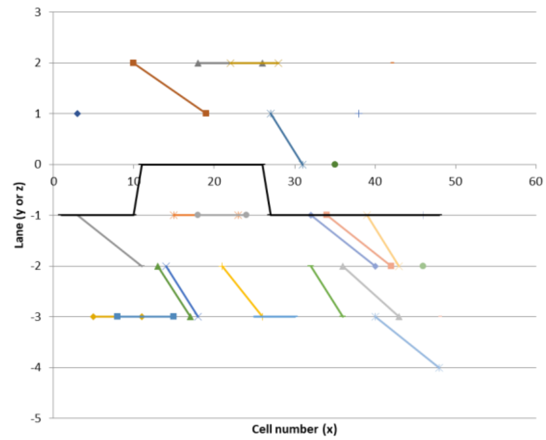

Figure 65b: Major - Police - left - 0.8 - 0.4 – Optimal

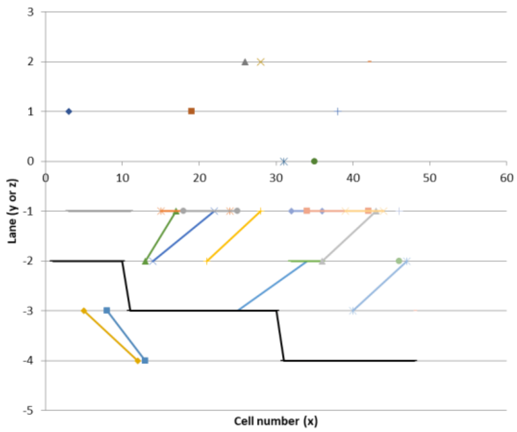

Figure 66a: Major - Police - middle - 0.8 - 0.4 – Heuristic

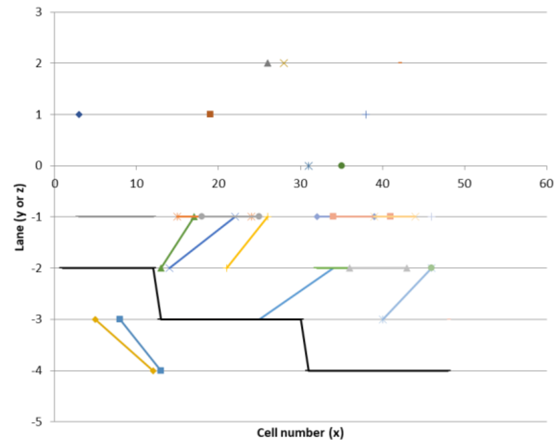

Figure 66b: Major - Police - middle - 0.8 - 0.4 - Optimal

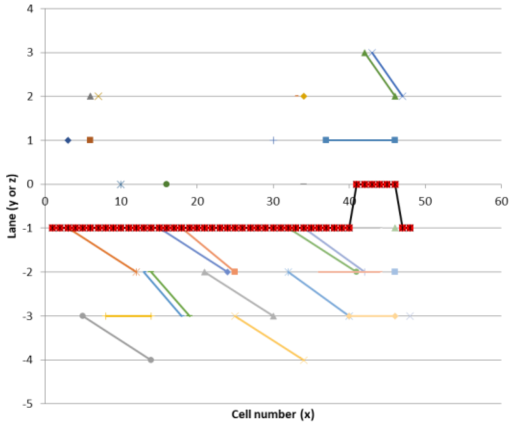

Figure 67a: Major - Police - left - 0.8 - 0.6 - Heuristic

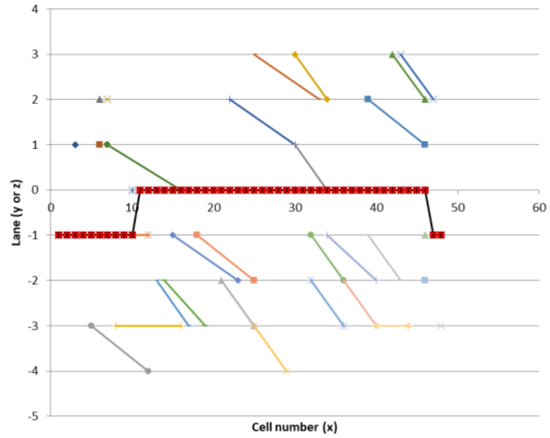

Figure 67b: Major - Police - left - 0.8 - 0.6 - Optimal

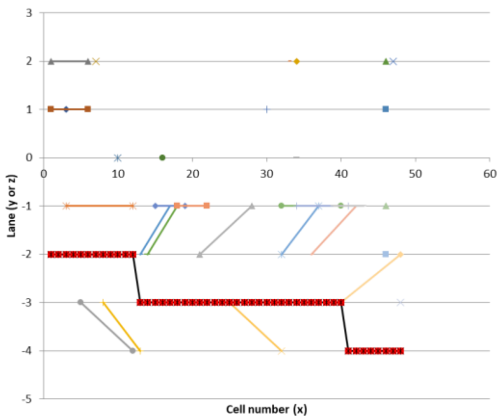

Figure 68a: Major - Police - middle - 0.8 - 0.6 – Heuristic

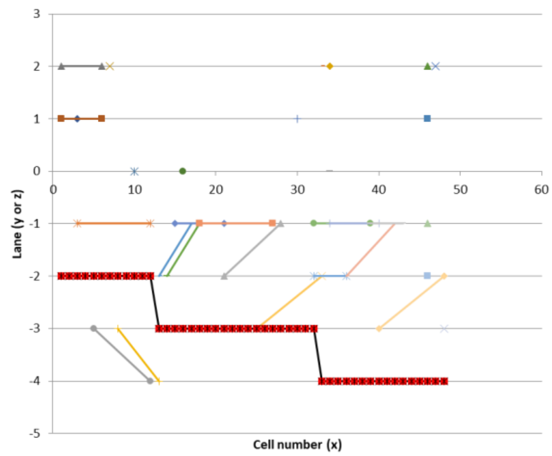

Figure 68b: Major - Police - middle - 0.8 - 0.6 - Optimal

REFERENCES

1. Wilde, Elizabeth Ty. "Do emergency medical system response times matter for health outcomes?" Health economics 22.7 (2013): 790-806.
2. Blackwell, Thomas H., and Jay S. Kaufman. "Response time effectiveness: comparison of response time and survival in an urban emergency medical services system." Academic Emergency Medicine 9.4 (2002): 288-295.
3. Pell, Jill P., et al. "Effect of reducing ambulance response times on deaths from out of hospital cardiac arrest: cohort study." Bmj 322.7299 (2001): 1385-1388.
4. Outcomes: Quantifying the impact of emergency response times, RapidSOS.com
5. Hannoun et al. “Facilitating Emergency Response Vehicles’ Movement through a Road Segment in a Connected Vehicle Environment.” (Ongoing)
6. Chiu, Yi-Chang, et al. "Evaluating regional contra-flow and phased evacuation strategies for Texas using a large-scale dynamic traffic simulation and assignment approach." Journal of Homeland Security and Emergency Management 5.1 (2008).
7. Kwon, Eil, and Sonia Pitt. "Evaluation of emergency evacuation strategies for downtown event traffic using a dynamic network model." Transportation Research Record: Journal of the Transportation Research Board 1922 (2005): 149-155.
8. Chen, Cheng-Chieh, and Chih-Sheng Chou. "Modeling and performance assessment of a transit-based evacuation plan within a contraflow simulation environment." Transportation Research Record 2091.1 (2009): 40-50.

9. Wolshon, Brian. "“One-Way-Out”: Contraflow freeway operation for hurricane evacuation." Natural hazards review2.3 (2001): 105-112.
10. Theodoulou, Gregoris, and Brian Wolshon. "Alternative methods to increase the effectiveness of freeway contraflow evacuation." Transportation Research Record: Journal of the Transportation Research Board 1865 (2004): 48-56.
11. Li, Qing, and Ziyou Gao. "Managing rush hour congestion with lane reversal and tradable credits." *Mathematical Problems in Engineering* 2014 (2014).
12. Yoo, Jae Bong, Jihie Kim, and Chan Young Park. "Road reservation for fast and safe emergency vehicle response using ubiquitous sensor network." 2010 IEEE International Conference on Sensor Networks, Ubiquitous, and Trustworthy Computing. IEEE, 2010.
13. Hausknecht, Matthew, et al. "Dynamic lane reversal in traffic management." Intelligent Transportation Systems (ITSC), 2011 14th International IEEE Conference on. IEEE, 2011.
14. Schouwenaars, Tom, et al. "Mixed integer programming for multi-vehicle path planning." Control Conference (ECC), 2001 European. IEEE, 2001.
15. Kaufman, David E., Robert L. Smith, and Karl E. Wunderlich. "An iterative routing/assignment method for anticipatory real-time route guidance." Vehicle Navigation and Information Systems Conference, 1991. Vol. 2. IEEE, 1991.
16. Levin, Michael W., and Stephen D. Boyles. "A cell transmission model for dynamic lane reversal with autonomous vehicles." Transportation Research Part C: Emerging Technologies 68 (2016): 126-143.

17. Toy, Charmaine, et al. "Emergency vehicle maneuvers and control laws for automated highway systems." IEEE Transactions on Intelligent Transportation Systems 3.2 (2002): 109-119.
18. Weinert, Florian, and Michael Düring. "Development and Assessment of Cooperative V2X Applications for Emergency Vehicles in an Urban Environment Enabled by Behavioral Models." Modeling Mobility with Open Data. Springer, Cham, 2015. 125-153.
19. “Traffic level of service calculation methods”, Appendix B, California CCAG
20. David Eck and Jim Ryan “The Chi-Square Statistic”, the Mathbeans Project http://math.hws.edu/javamath/ryan/ChiSquare.html